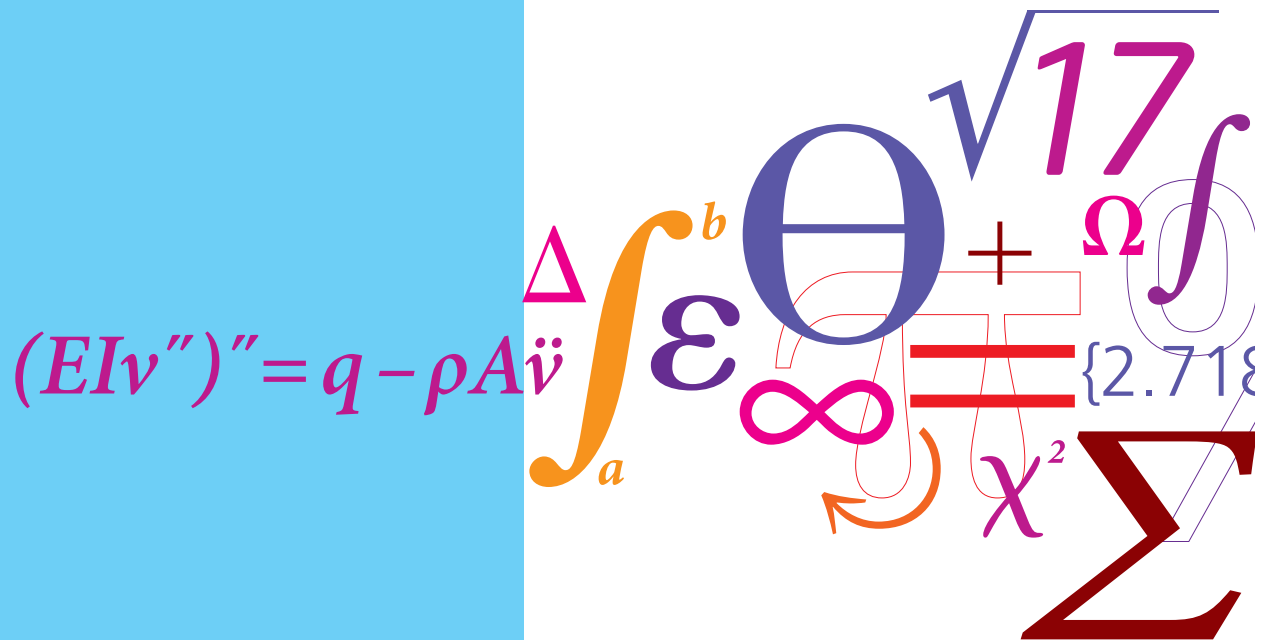


CFD Modelling of Combined Blast and Contact Cooling for Whole Fish

Master Thesis



Valur Oddgeir Bjarnason
May 2012



CFD Modelling of Combined Blast and Contact Cooling for Whole Fish

Master Thesis

By

Valur Oddgeir Bjarnason s100980

May 16th 2012

Section for Fluid Mechanics
Department of Mechanical Engineering
Technical University of Denmark

Supervisors

Dr. Jens Honore Walther, Associate Professor, DTU, Denmark

Dr. Björn Margeirsson, Research Group Leader, Matis, Iceland

Sigurjón Arason M.Sc., Chief Engineer, Matis, Iceland

Preface

This thesis consists of four main chapters: Introduction, Materials and methods, Results and Discussion. The Introduction presents the CBC-cooling method and how it effects fish quality and storage life. The Materials and methods chapter presents the experimental setup and which methods were applied to solve the CFD model. In the Results chapter the experimental results are presented and compared with the simulated results. Finally the Discussion chapter contains a review of the obtained results.

Combined blast and contact (CBC) cooling is a cooling method developed by the company *Skaginn ltd* (Akranes, Iceland) in cooperation with *Marel* (Garðabær, Iceland). The method is based on moving the product through a freezer tunnel where it is laid on an aluminum belt while cold air is blasted on its surface. The name of the cooler has been changed to *SuperChiller* but is referred to as *CBC-cooler* in this thesis.

The experimental results presented in this work are a part of the research and development project *Super-Chilled Round Fish - Pre Rigor*, which was funded by AVS R&D Fund of Ministry of Fisheries in Iceland. The financial support is gratefully acknowledged. Measurements were conducted in August and September, 2011 in cooperation with *Rekstrarfélagið Eskja ltd* (Hafnarfjörður, Iceland) which is a company equipped with a CBC-cooler.

I would like to express special gratitude to my main supervisor Dr. Jens Honore Walther for his good guidance and support throughout the project. Special thanks also to my two supervisors from *Matís*, Dr. Björn Margeirsson and Sigurjón Arason, for their great support and for giving me the opportunity of taking part in this research.

Fish quality is highly influenced by the cooling method which is applied during processing. Earlier research has shown that precooling whitefish fillets to a superchilled temperature in a CBC-cooler results in prolonged storage life. A CFD model which can simulate the effects of the CBC-cooling might save time and cost when predicting the necessary chilling time for a product when its thermal properties are known.

CFD models were created in two and three dimensions in *FLUENT* to simulate the superchilling process inside the CBC-cooler, and were compared with experimental results from two tests. The temperature inside the CBC-cooler and the chilling period for the first test were -7.4°C and 6 minutes, respectively. The corresponding values for the second test were -14.1°C and 14 minutes.

A thermal contact resistance between the aluminium belt and fish was determined to be $R = 0.028 \text{ m}^2 \text{ K/W}$ and the $k - \varepsilon$ RNG turbulence model was selected to simulate the air flow in the computational domain. These settings were obtained by comparison of simulated and experimental results from the first test (6 min in holding time at -7.4°C) and were used for all further simulations. The CFD model which simulated the settings in the second test resulted in a good comparison with measurements, although the temperature during the storage period resulted in an overestimation of temperature in the CFD model. Three meshes were compared and the one, which was most refined at the fish surface, generated the best results.

The three dimensional model was applied to the latter test to investigate if the height differences along the fish had an effect on the temperature distribution. The CFD model resulted in a good comparison, and showed that 3D effects were in place. The results at position 1 (45 mm above the belt, closest to the fish surface in contact with air) were better than for the 2D case, which included the finest grid.

A simulation of a 30 minute CBC-cooling and a storage period of one hour showed that the fish flesh did not reach initial freezing. Hence, it is assumed that a lower temperature or a longer chilling period needs to be applied for a whole fish of this size ($m \approx 2.5$ kg).

Contents

Preface	iii
Abstract	vi
1 Introduction	1
1.1 CBC-cooling of fillets	1
1.1.1 Storage Life	3
1.2 CBC-cooling of whole fish	4
1.3 Thesis Statement	5
2 Materials and methods	7
2.1 White fish properties	7
2.2 Temperature measurements	10
2.3 Numerical modelling	14
2.3.1 Geometry	14
2.3.2 Mesh generation	19
2.3.3 Governing equations	21
2.3.4 Solution procedure	23
2.3.5 Boundary conditions	25
2.3.6 Transient conduction	26
2.3.7 Thermal contact resistance	26
2.3.8 Near wall treatment	27
2.3.9 Error estimation	29

3	Results and discussion	31
3.1	Experimental results	31
3.1.1	Conventional CBC-cooler settings (Test 1)	32
3.1.2	Modified CBC-settings (Test 3)	33
3.2	Numerical results and comparison	37
3.2.1	Conventional CBC-cooler settings	37
3.2.2	Mesh refinement	41
3.2.3	Extended CBC-cooling with storage	45
3.2.4	3D results	51
3.2.5	30 minute CBC-cooling	54
3.2.6	Air flow comparison	55
4	Conclusions	59
	Bibliography	61
A	Test results from the project <i>Super-Chilled Round Fish - Pre Rigor</i>	67
A.1	Test 1	68
A.2	Test 2	70
A.3	Test 3	75
A.4	Test 4	78
A.4.1	Storage at Matis	83

Nomenclature

$2D$	Two dimensional
$3D$	Three dimensional
α	Proportion of frozen water in fish flesh
Δx	Thickness, [m]
ρ	Density, [kg/m ³]
C	Courant number, dimensionless
c_p	Specific heat, [kJ/(kg K)]
CBC	Combined blast and contact
CFD	Computational fluid dynamics
EXP	Experimental
H	Thickness of fish at cross section, [m]
k	Conductivity, [W/(mK)]
L	Full length of fish, [m]
L'	Length of the fish body, excluding tail and head, [m]
LC	Liquid cooling
NC	No cooling

PI	Plate ice
q	Heat flow per unit area, [W/m^2]
R	Thermal contact resistance, [$m^2 K/W$]
Re	Reynolds number, dimensionless
RMS	Root mean square
T	Temperature, [$^{\circ}C, K$]
t	Time, [s]
T_0	Initial temperature, [$^{\circ}C, K$]
T_{∞}	Free stream temperature, [$^{\circ}C, K$]
$T_{f,i}$	Initial freezing temperature, [$^{\circ}C, K$]
u_{∞}	Free stream velocity in x-direction, [m/s]
X'_W	Unfreezable water proportion
X_W^O	Total water proportion
X_W^u	Unfrozen water proportion
X_I	Ice proportion
y^+	Wall distance, dimensionless

CHAPTER 1

Introduction

Fish quality and hence, its value is mainly influenced by five factors: Handling, cooling, processing, packaging and storage. The storage life of fresh fish products is very limited and is therefore an important factor to take into account when the product is to be exported. In order to maintain fish freshness during exportation, temperature control inside the storage is very important. The Combined Blast and Contact (CBC) cooling method has resulted in prolonged storage life of fish fillets [Lauzon et al., 2010] and possibly for whole fish [Gao, 2007].

1.1 CBC-cooling of fillets

CBC-cooling is a processing technique developed by the company Skaginn ltd. (Akranes, Iceland). The technique is based on superchilling the product by transferring it through a freezer tunnel on a Teflon coated aluminium belt and simultaneously blasting cold air over it. The contact cooling is generated by the cooling energy accumulated in the aluminium belt. This cooling method which slightly freezes the skin in contact with the belt, without excessively freezing the flesh, has mainly been applied for cooling fillets, not whole fish. Superchilling, as used for preservation of food, implies temperatures in the borderline between chilling and freezing, i.e. slightly below the initial freezing point of the fish.

The CBC-cooling is considered a quick freezing process which results in good product quality. This is because food products in general contain a considerable amount of water and when the product is considered frozen, most of its water content has been turned into ice. Slow freezing causes the formation of large ice crystals which might cause damage to the cells in the biological material of the product. Quick freezing, such as the CBC-cooling,

results in small ice crystal formation and less damage to the product [Granryd, 2005]. The CBC-cooling delivers a stiff and robust product which makes cutting and trimming easier. Since the ice crystal formation is very small, its liquid remains inside the fish flesh. These advantages result in a product of great quality with increased storage life compared to other methods [Magnússon et al., 2009]. The main challenge in this process is to maintain a stable and a sufficiently low temperature, which often is more difficult for fresh food rather than frozen food.

It takes the fish fillets a period of 6 to 8 minutes to travel through the CBC-cooler. Before entering the cooler the fillets go through a pre-cooler/fluid-ice which contains approximately 2.5 % salt. This is done so the fillets can endure the CBC-cooling without excessively freezing the flesh. After the fish exits the cooler the temperature of the product equalizes in around 1-2 hours, because the outer parts (mainly the skin part) chill the warmer parts. Figure 1.1(a) shows fish fillets inside the CBC-cooler along with one of the fans used to blow air onto the fish. Figure 1.1(b) shows fish fillets exiting the CBC-cooler where they are dropped on a conveyor belt and transferred to skinning and trimming.

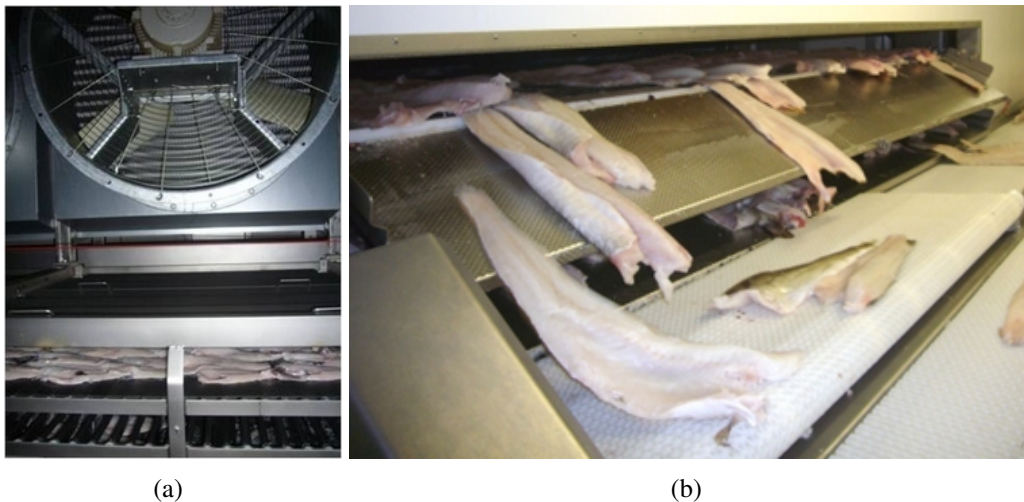


Figure 1.1: Inside the CBC-cooler, fillets are laid down on the skin and superchilled with blast and contact cooling (a). Fillets exiting a CBC-cooler, at a temperature around -1°C , and dropping on a conveyor belt which transfers them to skinning and trimming (b) [Valtýsdóttir et al., 2010].

Presented in Figure 1.2 is a flow graph of the basic steps in the cooling process of fish fillets before packaging and transportation to the market. The process starts at the capture of the cod on board the trawler where it is bled and packaged in ice or slurry ice. When the cod is received at the plant it is washed, gutted and graded before it is superchilled with the CBC-cooler.

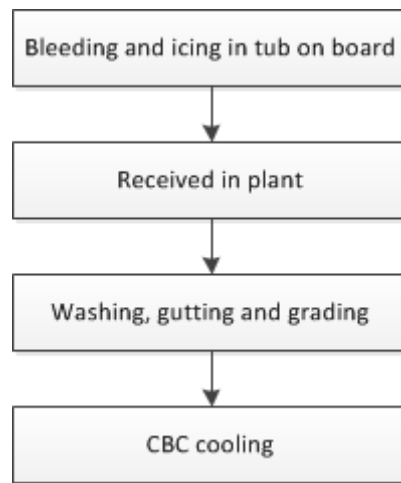


Figure 1.2: Flow graph of whole cod fish processed with CBC-cooling [Gao, 2007].

1.1.1 Storage Life

Fishing trips at sea may last from one to several days. Under conventional conditions (no CBC-cooling) the freshness period of cod (from catch) stored at about 0.5°C is 4 to 8 days [Lauzon et al., 2010]. Raw material age at processing and product temperature post-packaging are important parameters affecting the fish freshness and quality deterioration. Because of the insulation properties of EPS (expanded polystyrene) boxes generally used, CBC-cooling conducted before packaging is more efficient and will lead to a homogeneous product temperature once packed in the box. This stability in the product temperature, once packaged, is critical to maintain its freshness and to avoid undesirable quality defects [Lauzon et al., 2010]. When the fish reaches a uniform temperature below its initial freezing point of $T_{f,i} = -0.91^{\circ}\text{C}$ [Rahman, 2009] a higher amount of energy is needed to heat it to a temperature above $T_{f,i}$ than, e.g. if the product is heated from 1°C to 2°C . This is because of the effect of latent heat of melting in the fish flesh, as discussed later in Section 2.1.

According to sensory, microbiological and chemical analysis, from research done by Magnússon et al. [2009], adding CBC-cooling to the cooling process clearly results in a longer freshness period and storage life extension compared with the two groups of liquid cooling and no cooling where CBC-cooling was not applied. Temperature in the fish flesh was lower in the groups where CBC-cooling was applied at processing during the storage period. These results are compared in Table 1.1. The groups are defined as PI: Plate ice pre-cooling on board trawler, LC: liquid cooling, CBC: Combined blast and contact cooling at plant, NC: No cooling at plant and LI: Liquid ice pre-cooling on board trawler.

It is clear that when the CBC-cooling is applied to fish fillets the shelf life increases by

3-4 days and the freshness period by 1-2 days compared with liquid cooling and no cooling. The comparison in Table 1.1 shows that the CBC-cooling is an important cooling technique which can be used to gain and maintain the value of the product. The end of the freshness period is defined as when the fish has lost the freshness characteristics and reached the neutral phase (Torry score 7 out of 10). The end of the maximum shelf life period is when odour and flavour attributes (Torry score 5.5 out of 10) related to spoilage have become evident. The Torry scheme [Martinsdóttir et al., 2001] is used as an assessment of the fish flavour and odour with a scale from 1 to 10.

Table 1.1: *Freshness period and shelf life from catch according to sensory evaluation. The cod was processed two days post-catch [Magnússon et al., 2009].*

Group	Freshness period	Shelf life
PI, LC-CBC	6-8 days	14-15 days
PI, LC	6-7 days	9-12 days
PI, NC	5-8 days	8-11 days
LI, LC-CBC	8-9 days	15-16 days

Research performed by Martinsdóttir et al. [2004, 2005] showed that CBC-cooling slows down the deterioration process significantly compared with conventional processing. By processing the the raw material one day from catch, a storage life of 13 days was obtained for cod fillets stored at 0.5 °C.

By working with the raw material three days from catch, a storage life of 14 days was obtained for cod fillets stored in EPS boxes at 0.5 °C. Two days may be added to this storage life if the storage temperature is lowered from 0.5 °C to –1.5 °C [Olafsdóttir et al., 2006]. The storage temperature needs to be stable and close to –1.5 °C and –1.0 °C in order to obtain the optimal storage for fish fillets.

Applying the CBC-cooling and storing the fish at 0.5 °C results in an overall sensory shelf life of 12.5 to 14 days. When stored at –1.5 °C after the CBC-cooling, the storage life is extended to at least 15 days. This shelf life extension is of high economical value because it allows distant transportation of fresh fish by ship or truck, which is less expensive compared to air freight [Olafsdóttir et al., 2006].

1.2 CBC-cooling of whole fish

The idea behind using the CBC-cooling technique on whole fish is to move the process shown in Figure 1.2 into the trawlers where the fish is caught. The largest amount of information available about CBC-cooling of whole cod fish is found in research done by Gao [2007]. In this research, CBC-cooling is compared with pre-cooling with slurry ice and usage of cooling mats/packs. The cooling time of the CBC-cooler was fixed

at 11 minutes for all experiments. Two sets of experiments were made where different temperature settings were applied.

From the first experiment, conducted on December 8th, it was recommended that the cooling time of 11 minutes should be extended to decrease the central temperature down to -1°C and that the air temperature should be in the range of -20°C to -10°C for whole cod with average weight around 1 kg.

From the second experiments, conducted on January 30th, it was concluded that an approximate air temperature should be in the range of -23°C to -20°C for whole cod with an average weight around 1 kg, when cooled in a CBC-cooler for 11 minutes. A different chilling time would result in different temperatures.

Results where CBC pre-cooling is compared with slurry ice and the use of cooling mats/packs show that CBC-cooling is a good method for delaying quality deterioration of fresh cod fillets with regards to chemical and microbiological assessments. Careful temperature monitoring in further chilled storage should be maintained to guarantee the fresh fish quality [Gao, 2007].

1.3 Thesis Statement

The main purpose of this work is two fold: (1) Conduct experiments to determine the required setting in the CBC-cooler which cause superchilling of the flesh for whole fish, and (2) to generate CFD models in 2D and 3D to simulate the temperature behaviour inside a whole cod fish during CBC-cooling and the storage time. The simulated results are compared with experimental results. Results and settings used in this model can be implemented for future simulations involving the CBC-cooling method, e.g. when introducing other fish species, such as salmon or when predicting longer cooling periods.

Materials and methods

In this chapter the materials and methods used in the study are described. Firstly the thermal properties of white fish are presented, i.e. how the thermal conductivity and specific heat vary with temperature. Secondly temperature measurements are described by describing the placement of temperature data loggers inside and outside of the fish flesh along with the position of the anemometer used for recording air velocity inside the CBC-cooler. Lastly the theory and boundary conditions used for calculating the solution are presented.

2.1 White fish properties

When predicting the time necessary for cooling or heating of food products, information on its thermal properties are of high importance. In order to obtain superchilling of the product, its core temperature must get below the products initial freezing temperature, $T_{f,i}$. The fish product examined in this thesis is cod (*Gadus morhua*), which is one type of white fish.

The initial freezing temperature ($T_{f,i}$) of cod is listed as $-0.91\text{ }^{\circ}\text{C}$ by Fikiin [1998]. In research done by Margeirsson et al. [2012] a value of $T_{f,i} = -0.92\text{ }^{\circ}\text{C}$ was adopted in the *FLUENT* models because of a better fit with experimental data. The same value of $T_{f,i}$ is adopted in this study. When a product is cooled below its initial freezing temperature ($T_{f,i}$), phase change of the water inside the fish muscle begins along with formation of ice crystals. According to Fikiin [1998] the total proportion of water within the fish flesh is 80.3 %.

Figure 2.1 presents enthalpy as a function of the total amount of water within the fish

flesh where α is the amount of frozen water in the fish [Rha, 1975]. A close inspection of the figure shows that the difference between cooling fresh fish down to around -1.4°C compared to around -1.0°C is larger than one might expect. For cod, with 80.3% water content, around 30-40% of the flesh is frozen at -1.4°C compared to around 15% at -1.0°C . Freezing around 30-40% of the water content may cause irreversible changes to the product chemical properties. The area of interest is highlighted with a red circle in the figure.

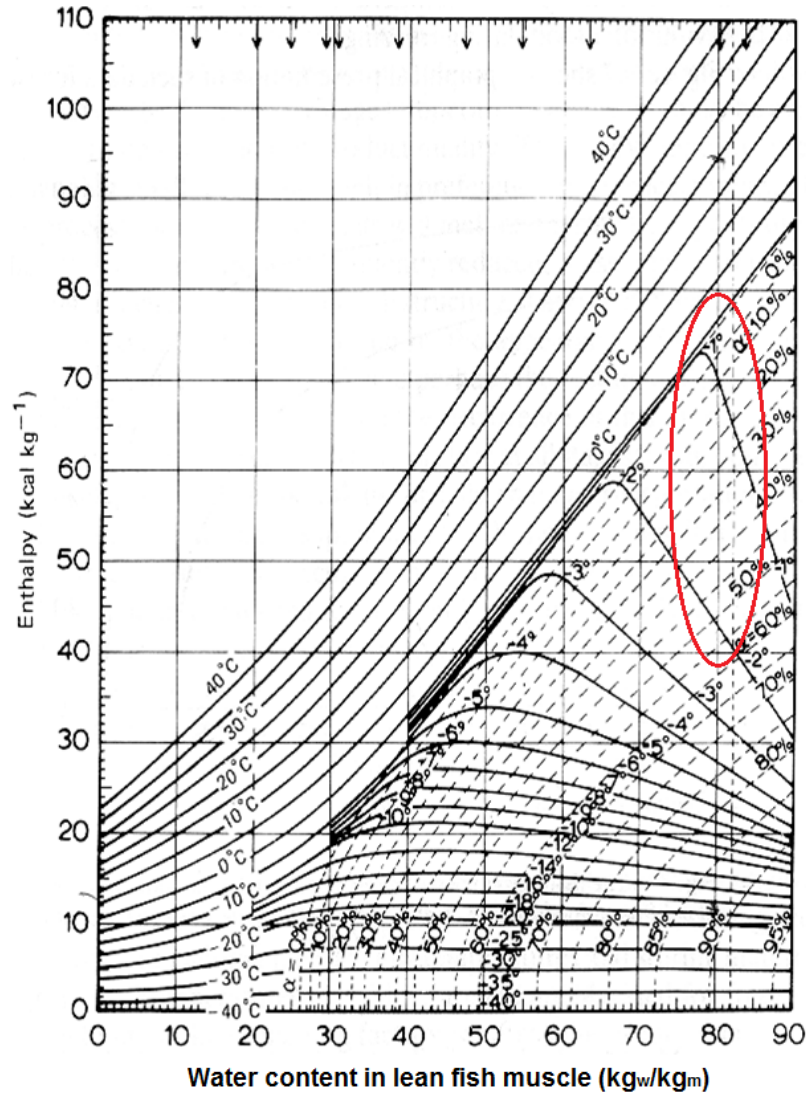


Figure 2.1: Enthalpy diagram for lean fish muscle [Rha, 1975] where α represents the percentage of frozen water in the fish flesh.

Rahman [2009] presents four different types of water in frozen foods: total water (X_W^0), ice

(X_I), unfreezable water (X'_W) and unfrozen water (X''_W). Total water can be written as

$$X_W^O = X''_W + X_I + X'_W \quad (2.1.1)$$

Since not all water in the product is freezable, a good prediction for the amount of ice content is achieved by

$$X_I = (X_W^O - X'_W) \left(1 - \frac{T_{f,i}}{T}\right) \quad (2.1.2)$$

with $T_{f,i} = -0.91^\circ\text{C}$ and $(X_W^O - X'_W)$ as the total freezable water. Unfreezable water, expressed in kilograms of unfreezable water per kilogram of sample or dry solids, is defined as:

$$X'_W = B(1 - X_W^O) \quad (2.1.3)$$

where the proportion of unfreezable or bound water, according to Fikiin [1998], is $B = 0.278$. The function in equation 2.1.2 is presented visually in Figure 2.2 with the initial freezing temperature of $T_{f,i} = -0.91^\circ\text{C}$ at the far right. The figure illustrates that even when the fish is cooled down to -40°C , the proportion of frozen flesh is only 72%. The figure also shows that from the initial freezing temperature of $T_{f,i} = -0.91^\circ\text{C}$ to a temperature of $T = -5^\circ\text{C}$ the ratio of frozen water proportion rises from 1% to 61%, respectively.

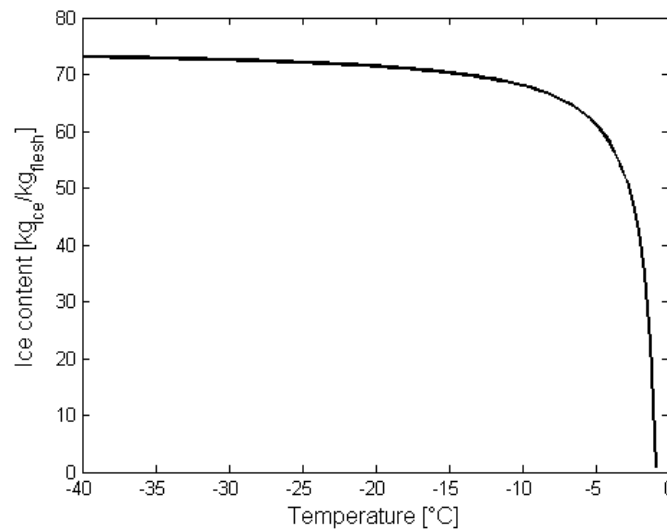


Figure 2.2: Frozen water in fish flesh as a function of temperature.

Table 2.1 presents how the thermal conductivity (k) and specific heat (c_p) of cod change with temperature.

Table 2.1: Temperature dependent thermal properties of cod [Johnston et al. [1994], Zueco et al. [2004]].

T [°C]	-4	-3	-2	-1	-0.92	0	5	10
k [W/(mK)]	1.361	1.341	1.322	1.302	1.302	0.430	0.430	0.430
c _p [kJ/kgK]	15.11	26.54	65.64	102.7	223.0	4.144	3.641	3.683

The constant density of $\rho = 1054 \text{ kg/m}^3$ and the thermal conductivity presented in Table 2.1 are adopted from Zueco et al. [2004].

The data presented in Table 2.1 along with Figures 2.2 and 2.1 show a strong variation, with respect to temperature properties, in the fish flesh when it is cooled down to its initial freezing temperature of $T_{f,i} = -0.91 \text{ }^\circ\text{C}$, and lower.

2.2 Temperature measurements

Temperature measurements are performed for thirteen different cases where each case consists of measurements of three whole fish samples. Ibutton temperature loggers (DS1922L) from Maxim Integrated Products (Sunnyvale, CA, USA) are used to monitor temperature inside the fish flesh and the free stream temperature. The Ibutton temperature loggers have a resolution of $0.0625 \text{ }^\circ\text{C}$, measurement range of $-40 \text{ }^\circ\text{C}$ to $85 \text{ }^\circ\text{C}$ and an accuracy of $\pm 0.5 \text{ }^\circ\text{C}$ between $-15 \text{ }^\circ\text{C}$ and $65 \text{ }^\circ\text{C}$.

The air velocity is measured with a Thermo-Anemometer Data logger (model 451126) from Extech Instruments (Waltham, MA, USA). The anemometer has a resolution of 0.01 m/s , measuring range of $0.3 - 45 \text{ m/s}$ with an accuracy of $\pm (3\% + 0.1) \text{ m/s}$.

The temperature data loggers are inserted in the manner shown in Figure 2.3. A cut is made through the flesh where the data loggers are to be placed. Three data loggers are inserted in cross section *C* (location of the cross section is shown in Figure 2.4) one above the spine and two below, closer to the belt. See vertical placements of temperature data loggers in Figure 2.5.

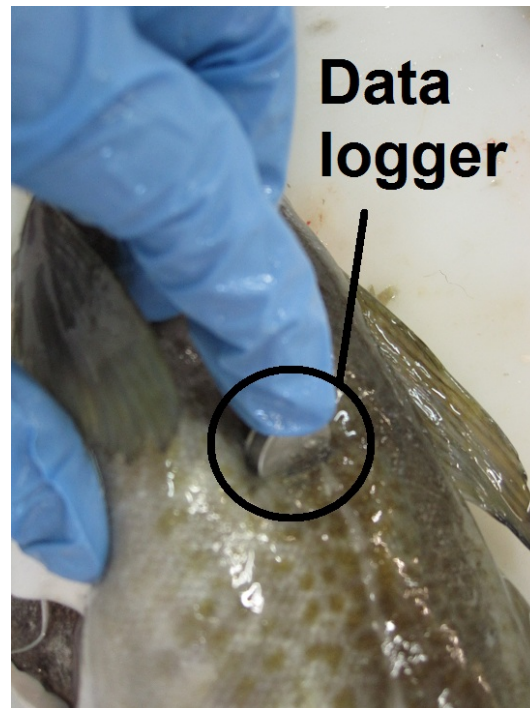


Figure 2.3: *Temperature data logger inserted into the cod.*

The fish samples used for modelling are measured in cross sectional locations noted by *A*, *B* and *C*, as shown in Figure 2.4. In each of those locations the thickness and width are measured. Here, L is the total length of the fish and L' is the total fish length, excluding tail and head.

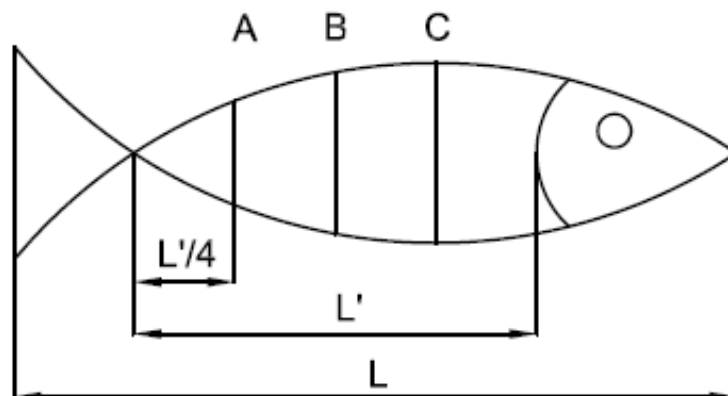


Figure 2.4: *A schematic image of a cod.*

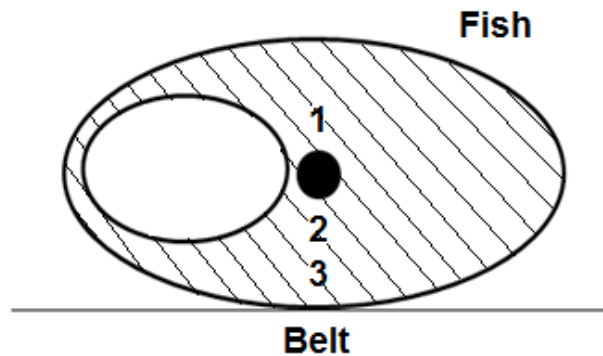


Figure 2.5: Cross section of cod with placement of temperature data loggers.

The free stream temperature is measured with the settings shown in Figure 2.6(a) where a temperature data logger is suspended from a beam close to the aluminium belt. The anemometer, used to measure the air velocity close to the fish, is fastened as shown in Figure 2.6(b). Average values of the air velocity and temperature are calculated using the data obtained from these measurements. This averaging makes it simple to insert single values for the inlet velocity and temperature in the CFD-model.

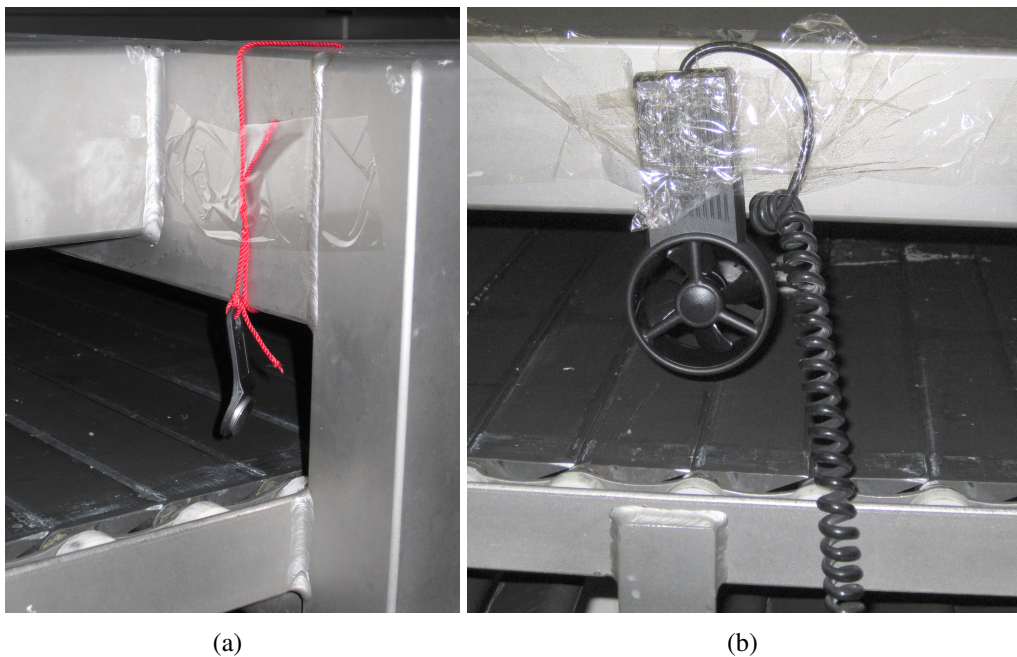


Figure 2.6: Setup of experimental equipment for environment measurements. Temperature data logger (a) and anemometer (b).

To show why an average value for the velocity is selected, Figure 2.7 is presented. The horizontal line represents the average velocity used for the conventional CBC-cooling, as presented later in Section 3.1.1. The measured velocity ranged from approximately 2.2 m/s to 3.2 with large fluctuations in between. Since an average value for the air velocity and temperature are used in the model a reason for possible errors is introduced.

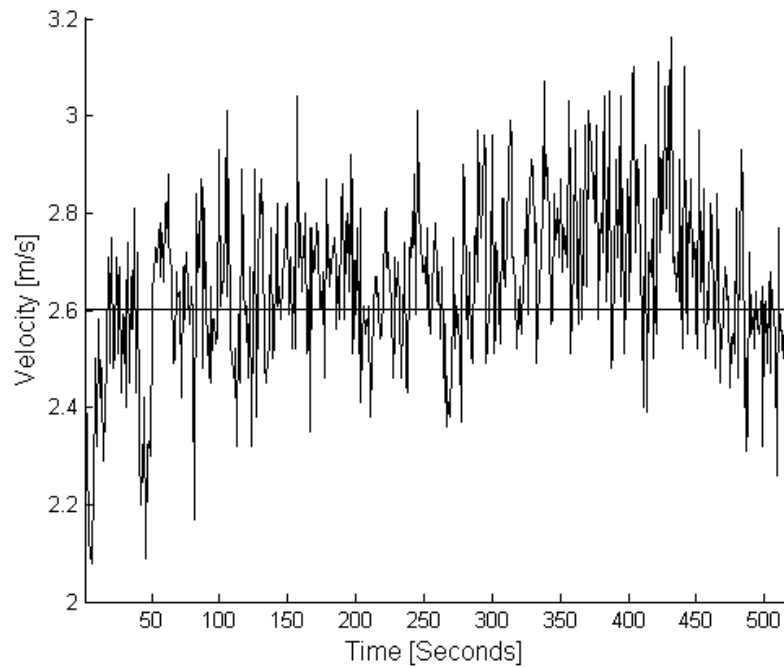


Figure 2.7: Measured air velocity (m/s) for a period of 500 s.

After the CBC-cooling the fish is placed in an EPS box as shown in Figure 2.8(a). During the CBC-cooling the EPS boxes are stored inside a chilled storage room in order to get the box temperature closer to the fish temperature (see Figure 2.8(b)). The box is closed and stored in the same chilling storage as mentioned before for 1 to 1.5 hours.



Figure 2.8: Cod inside the EPS box after CBC-cooling (a). EPS boxes stacked on a pallet inside the chilled storage (b).

2.3 Numerical modelling

Two finite volume models, in two and three dimensions, are developed using the commercial Computational Fluid Dynamics (CFD) software *FLUENT*. The calculated results obtained by these models are compared with the experimental results.

2.3.1 Geometry

Two geometrical models are created, one is a two dimensional cross section of a fish at position *C* (See Figure 2.4) and the other is a three dimensional model of an almost whole fish. Both models also include an aluminium belt and the air domain surrounding the two bodies. These three parts are necessary factors for simulation of the whole process.

Figures 2.9 and 2.10 are taken into account when creating the models. These two figures are only examples of the fish used for the experiments and are not the exact samples used when creating the CFD models. Figure 2.9 is also used to illustrate that the fish shape is very complex and difficult to model. The two most important parts of the model are the surface where the air hits the fish and the area of contact between the fish and the aluminium belt. The air hits the fish from the right, in the CBC-cooler, with respect to Figure 2.10.



Figure 2.9: A sample of a cod which is used for comparison when generating the CFD model.



Figure 2.10: Cod seen from the tail.

Two dimensional model

The 2D model is created with respect to measurements made at cross section *C* (see Figure 2.4). An important part of the model is the section of the cod which is in contact with the aluminium belt. It is quite difficult to measure the size of this section so it has to be estimated, taking Figure 2.10 into account. The generated 2D model of the cod is shown in Figure 2.11 with its main dimensions. The cod is only one of three parts within the computational domain. The other parts are the surrounding air, with dimension $500 \times 200 \text{ mm}$, and the belt on which the cod is placed with dimensions $500 \times 10 \text{ mm}$. This computational domain is a cross section of the domain shown in Figure 2.14, at the location of cross section *C*.

As noted before the temperature is measured at three locations in the fish flesh (see Figure 2.5) with temperature data loggers. The exact location of these data loggers within the cross section is difficult to determine by measurements. The data logger locations are determined by inserting a number of temperature monitors in the cross section of the CFD model, as shown in Figure 2.11. The three monitors that give the best results compared

with experiments are used in comparison. It should be noted that the position of these monitors vary for different fish specimen since the data logger locations within each fish are never exactly the same.

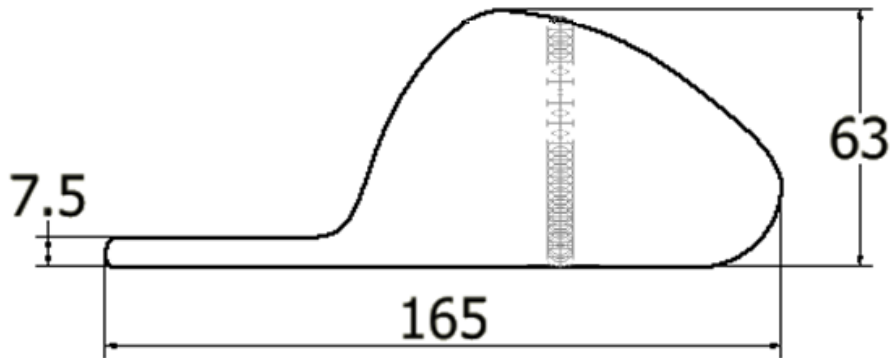


Figure 2.11: 2D model of the cod with dimensions (mm) and placement of temperature monitors.

The temperature from each monitor is stored after a pre-defined number of time steps and written in a *.out* file which is used for post-processing. The temperature values are obtained by applying a vertex average to each cell. *The vertex average of a specified field variable on a surface is computed by dividing the summation of the vertex values of the selected variable by the total number of vertices* [ANSYS, 2009].

Three dimensional model

The main reason for making the model in 3D is to see if the thickness variations along the length of the cod (z-direction) result in different effects on the temperature gradients in cross section *C* compared with the 2D model. The height and width measurements of cross sections *A*, *B* and *C* and the measured lengths between the cross sections ($L/4$) are used to produce a 3D model. The 3D model is generated by using the *Loft* feature where the geometry of a number of aligned cross sections are used to create a solid body. The generated geometry is shown in Figures 2.12 and 2.13.

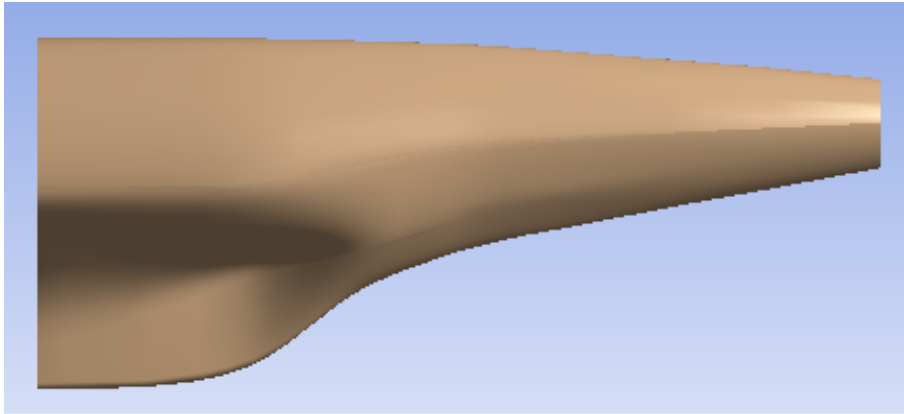


Figure 2.12: *3D model of cod used for calculations.*

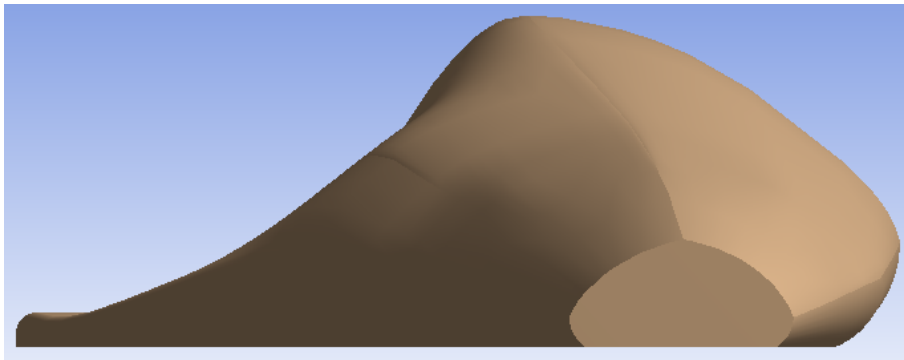


Figure 2.13: *3D model of cod seen from the tail.*

The control volume used for the 3D-calculations is shown in Figure 2.14 along with its dimensions. The length of the fish in the model corresponds to the length L' , as defined in Figure 2.4

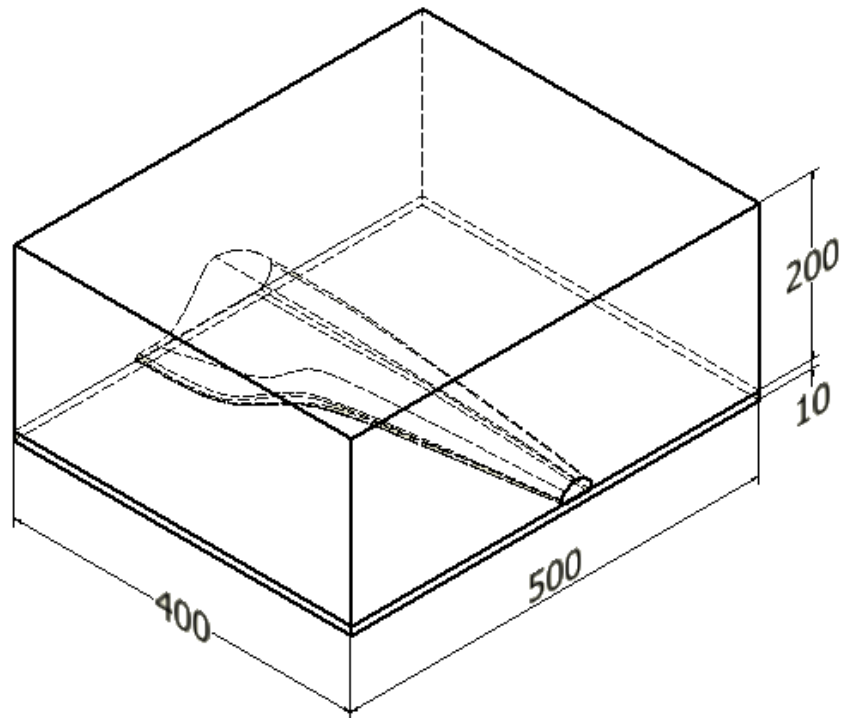


Figure 2.14: 3D model of the computational domain, including its dimensions (mm).

The area of contact between fish and aluminium belt has a large influence on the thermal conduction between the two bodies. Figure 2.15 shows the contact area in the CFD model and the position of cross section C.



Figure 2.15: The area of contact between fish and aluminium belt with a vertical line showing the position of cross section C.

2.3.2 Mesh generation

The meshes for the 2D and 3D cases are generated with two different cell types. The 2D mesh consists of quadrilateral cells, as shown in Figure 2.16(a), and the 3D mesh consists of tetrahedral cells, as shown in Figure 2.16(b).

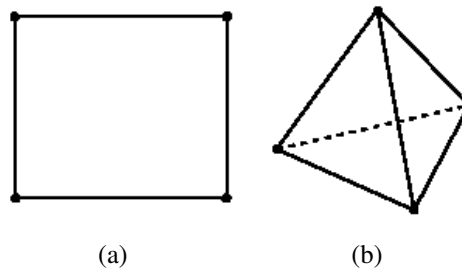


Figure 2.16: The two different cell types used to generate the meshes. Quadrilateral (a) and tetrahedral (b).

One of the parameters which needs to be taken into account when generating a mesh is if the cells are skewed. Skewness is defined by ANSYS [2009] as *the difference between the shape of the cell and the shape of an equilateral cell of equivalent volume*. If the cells are highly skewed they can decrease accuracy or cause divergence when the solution is calculated.

Two dimensional model

Since the geometry for the 2D case is not of high complexity, quadrilateral cells are used for the mesh generation, as mentioned before. Three types of meshes are generated: Mesh 1 which consists of around 18,000 cells, Mesh 2 containing around 120,000 cells and Mesh 3 which is comprised of around 130,000 cells. Mesh 2 is a refined version of Mesh 1, used to examine the possible gains of a finer mesh. Mesh 3 is the same as Mesh 2 but with a refined grid at the fish surface adjacent to air. The smallest cells in the mesh are positioned along the edges of the cod. This is to capture the heat extraction from the fish to the environment caused by forced convection and contact cooling.

Meshes 1 and 2 are compared in Figures 2.17(a) and 2.17(b), respectively. The two figures show that Mesh 2 is significantly finer than Mesh 1, one might therefore expect better results with the finer mesh.

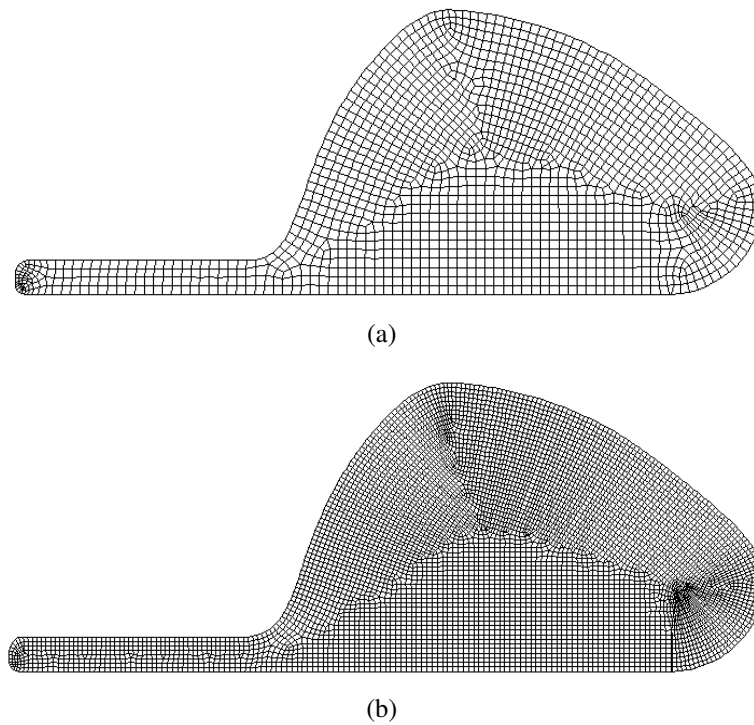


Figure 2.17: Comparison of the fish domain meshes. Mesh 1 (a) and Mesh 2 (b).

Mesh 2 is refined further at the fish surface in order to obtain a y^+ value closer to 5, which is the intersection of the viscous sublayer and the buffer layer (see Section 2.3.8). Mesh 3 is compared with Mesh 2 close to the fish surface in Figure 2.18.

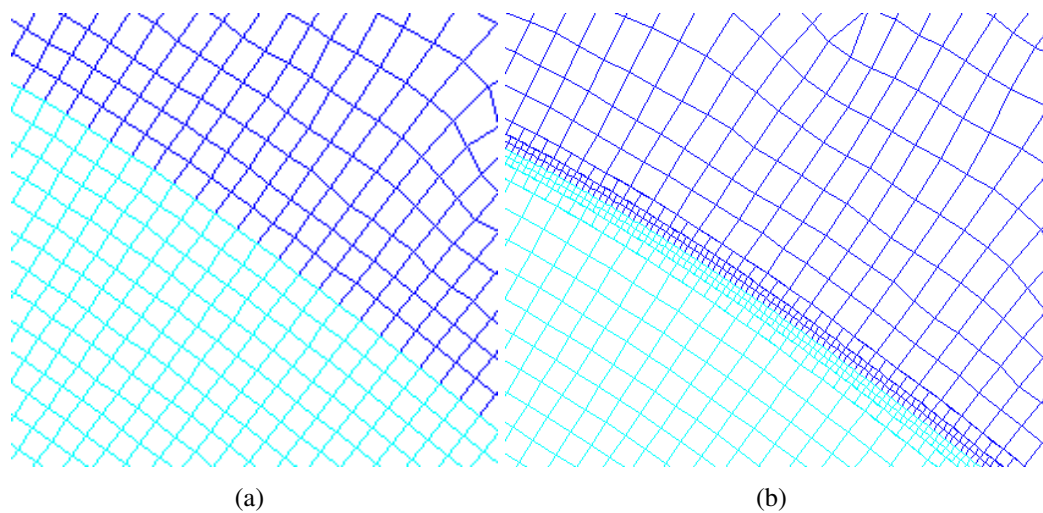


Figure 2.18: Comparison of Meshes 2 and 3 at the fish surface. Mesh 2 (a) and Mesh 3 (b).

Three dimensional model

The 3D case consists of a semi-full fish model which is complex in shape. It is therefore not the best option to use a mesh of quadrilateral cells. The selected cells for this case are tetrahedral which are easily adjusted to the defined geometry. The 3D mesh of the fish, seen from above, is presented in Figure 2.19. The whole computational domain consists of a total of approximately 1,345,000 elements which is significantly higher than for the finest 2D mesh (Mesh 3).

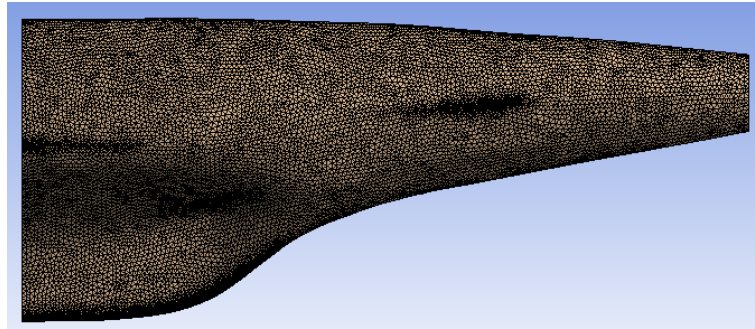


Figure 2.19: *Mesh of the 3D model seen from above.*

A cross section of the mesh in 3D is shown in Figure 2.20. When this cross section is compared with the 2D cross section of Mesh 2 (see Figure 2.17(b)), it is clear that the 2D mesh is finer. The 3D mesh might therefore not return results as accurate as the 2D meshes. The main purpose of the 3D case is to see if there are any longitudinal cooling effects obtained in the fish flesh.

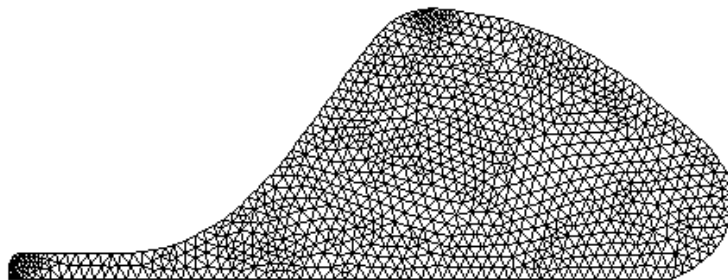


Figure 2.20: *Mesh of the 3D model seen from the fish head.*

2.3.3 Governing equations

This section introduces the governing equations used to solve the fluid flow and heat transfer inside the computational domain. The flow field behaviour in the models is

obtained by solving the continuity and momentum equations in 3D. The energy equation is solved to compute the transient temperature change of the complete computational domain. To approximate how the air behaves as it flows around the fish the three governing equations are solved within each element of the computational domain.

Continuity

The boundary layer flow field along the surface of the fish and belt is predicted by solving the equations that express conservations of mass and momentum in the boundary layer.

The continuity equation which expresses conservation of mass for an incompressible fluid is defined as

$$\nabla \cdot \mathbf{V} = \frac{\partial u}{\partial x} + \frac{\partial v}{\partial y} + \frac{\partial w}{\partial z} = 0 \quad (2.3.1)$$

assuming that the density is constant along each streamline. Equation 2.3.1 is called the three dimensional continuity equation for incompressible flow, because it expresses mathematically the fact that the flow is continuous.

Navier-Stokes equation

Conservation of momentum in an inertial reference frame is described by the Navier-Stokes equation. The turbulence is included by introducing a turbulent inertia tensor $\overline{u'_i u'_j}$ and a mean Navier-Stokes equation is obtained:

$$\rho \frac{D\bar{V}}{Dt} = \nabla \bar{p} + \nabla \cdot \tau_{ij} \quad (2.3.2)$$

where \bar{p} is the static pressure and

$$\frac{D}{Dt} = \frac{\partial}{\partial t} + (\mathbf{V} \cdot \nabla) \quad (2.3.3)$$

Note that the gravitational forces are neglected. The stress tensor τ_{ij} is given by

$$\tau_{ij} = \underbrace{\mu \left(\frac{\partial u_i}{\partial x_j} + \frac{\partial u_j}{\partial x_i} \right)}_{Laminar} - \underbrace{\rho \overline{u'_i u'_j}}_{Turbulent} \quad (2.3.4)$$

where μ is the molecular viscosity. Here the Einstein summation is used, where $u_i = (u_1, u_2, u_3) = (u, v, w)$.

Energy equation

By applying the law of conservation of energy and the Fourier's law of heat conduction on a differential volume and taking the limiting case of this as volume goes to zero, one arrives at the general equation for thermal energy transport, defined as:

$$\rho c_p \frac{D\bar{T}}{Dt} = -\frac{\partial}{\partial x_i} (q_i) + \bar{\Phi} \quad (2.3.5)$$

where

$$\bar{\Phi} = \frac{\mu}{2} \overline{\left(\frac{\partial \bar{u}_i}{\partial x_j} + \frac{\partial u'_i}{\partial x_j} + \frac{\partial \bar{u}_j}{\partial x_i} + \frac{\partial u'_j}{\partial x_i} \right)^2} \quad (2.3.6)$$

and

$$q_i = \underbrace{-k \frac{\partial \bar{T}}{\partial x_i}}_{\text{Laminar}} + \underbrace{\rho c_p \overline{u'_i T'}}_{\text{Turbulent}} \quad (2.3.7)$$

The velocities u , v and w can be obtained by solving Equation 2.3.2 [White, 2006]. Note that within the fish cross section the specific heat, c_p , and conductivity, k , are functions of temperature as defined in Section 2.1.

The equations of continuity, momentum and energy can be made dimensionless by redefining the dependent and independent variables as dimensionless. This is done by dividing the variables by constant reference properties which apply for the flow. By substitution of these dimensionless numbers into the energy equation and rearranging the equation, one of the dimensionless parameters obtained is the Reynolds number. The same number is obtained by substituting dimensionless parameters into the Navier-Stokes equation [White, 2006]. The Reynolds number is defined as:

$$Re = \frac{H u_\infty}{\nu} \quad (2.3.8)$$

Here, the length parameter H is the height of the fish at cross section C , as defined in Figure 2.11. With the air inlet velocity, $u_\infty = 2.6$ m/s and the kinematic viscosity at -7.4°C as $\nu = 1.26 \times 10^{-5}$ m²/s a Reynolds number of 13,000 is obtained. According to Lienhard IV and Lienhard V [2010] turbulent behaviour for a circular cylinder in cross flow occurs for values of Re above 150. Since, in this case, $Re = 13,000$ the air flow is considered turbulent.

2.3.4 Solution procedure

The solution obtained by the commercial CFD code *FLUENT* is solved using a pressure based solver. The pressure based solver uses an algorithm where mass conservation of the velocity field is achieved by solving a pressure equation. The pressure equation is derived

from the continuity and momentum equations so that the velocity field, corrected by the pressure, satisfies continuity. The governing equations are non-linear and coupled to one another. Hence, a solution is obtained by iterating the entire set of governing equations until convergence is obtained [ANSYS, 2009, p. 642].

FLUENT converts the general scalar transport equation to an algebraic equation which can be solved numerically by using the finite volume technique. This technique involves approximating the integral with a sum and using interpolation to obtain the required face value.

Discretisation of the governing equations on a given two dimensional triangular cell, for a scalar quantity, ϕ , may be expressed as

$$\frac{\partial \rho \phi}{\partial t} V + \sum_f^{N_{faces}} \rho_f \vec{v}_f \phi_f \cdot \vec{A} = \sum_f^{N_{faces}} \phi \nabla \phi_f \cdot \vec{A}_f + S_\phi V \quad (2.3.9)$$

where N_{faces} is the number of faces enclosing the cell, ϕ_f is the face value of ϕ , $\rho_f \vec{v}_f \cdot \vec{A}$ is the mass flux through the face, \vec{A} is the face area, $\nabla \phi_f$ is the gradient of ϕ at the face and V is the cell volume. The time dependent value of $\frac{\partial \rho \phi}{\partial t} V$ is a part of the temporal discretisation.

Spatial discretisation

By default *FLUENT* stores discrete values of the scalar, ϕ , at the center of each cell. In order to determine the convection terms in Equation 2.3.9, face values (ϕ_f) are required and must be interpolated from the cell center values. This is done by using an upwind scheme, or in this study a second order upwind scheme.

Upwind means that the face value ϕ_f is determined from cell values that are upstream with regards to the direction of the normal velocity v_n (see Equation 2.3.9). Since high accuracy is preferred to the solution, a second order upwind scheme is selected. This scheme computes cell face quantities by applying a multidimensional linear reconstruction which uses a Taylor series expansion to achieve high-order accuracy. The face value, ϕ_f , is computed using the following expression:

$$\phi_f = \phi + \nabla \phi \cdot \vec{r} \quad (2.3.10)$$

where ϕ and $\nabla \phi$ are the cell-centered value and its gradient in the upstream cell and \vec{r} is the distance from the upstream centroid to the face centroid. The gradient $\nabla \phi$ is determined by the *Least squares cell-based* method where the solution is assumed to vary linearly.

Temporal discretisation

Discretisation of the governing equations (Equations 2.3.1 to 2.3.5) in both space and time is very important for transient simulations. When the temporal discretisation is applied, the

differential equations are integrated over a time step Δt . The time derivative is discretised by using second order discretisation.

The governing equations are linearised in the CFD code either in an *implicit* or *explicit* form. For the implicit form, which is selected in this case, the unknown value in each cell for a given variable, is computed where relation between known and unknown values from the neighbouring cells are used. Each unknown value will therefore appear in more than one equation in the system. To get a solution these equations must be solved simultaneously by iteration [ANSYS, 2009, p. 641-673].

The time step, Δt , used when calculating the solution needs to be adjusted with respect to the dimensionless Courant number in the fluid domain. The Courant number is defined as

$$C = \frac{\Delta t \cdot u_{\infty}}{\Delta x_{cell}} \quad (2.3.11)$$

where Δx_{cell} is the width of the smallest fluid cell and u_{∞} is the free stream fluid velocity in the x-direction.

The system, which is solved with an implicit solver, requires that, for a stable and efficient calculation, the Courant number should not exceed a value of 20-40 in the most sensitive regions of the domain [ANSYS, 2009]. Looking at Equation 2.3.11 one can see that when the the mesh is refined the time step needs to be decreased to a value according to the width of the smallest fluid cell.

2.3.5 Boundary conditions

In order to generate good results, which show a good comparison, appropriate boundary conditions must be applied to the computational domain. The most important settings, such as the inlet velocity, the initial temperature and the air temperature, are obtained by measurements as described in Section 2.2.

The fish is assumed to be at uniform initial temperature, T_0 . The air flow is considered incompressible and uniform at the inlet of the control volume, representing the fans blowing in the air. The air temperature at the inlet is considered constant and expressed with T_{∞} . Under real circumstances the temperature and velocity fluctuate during the cooling period (see Figure 2.7).

Since the CBC-cooling is a low temperature process which takes place within a closed space, radiation effects are neglected.

The boundary conditions at the outlet and top wall of the control volume are set as pressure outlets with a constant temperature of T_{∞} . A turbulence intensity of 10 % and a length scale of 1 cm is used within the fluid domain.

A coupled boundary condition is applied between the air and fish surface, as well as between the air and belt. This boundary condition allows interaction between the fluid and solid zones, or in this case heat transfer.

The 2D model is in fact a 3D model with symmetric boundary conditions at the view planes. The 2D model, therefore, simulates a fish with uniform thickness out of and into the view plane. This means that the effect of thickness and geometry change along the fish has no influence on the solution.

The solution for the modified CBC-cooler settings is calculated in two parts in *FLUENT*. The modified CBC-cooling conditions are applied for a period of 14 minutes. After the CBC-cooling the air flow is cut off and set to 0 m/s and adiabatic boundary conditions (no heat flux) are applied to the four surrounding walls because the good insulation of the EPS box.

2.3.6 Transient conduction

Transient conduction is defined as the mode of thermal energy flow within an object, in which temperatures change in time. During the transient conduction period, temperatures within the system will change in time towards a new equilibrium. Once equilibrium is reached, heat flow into the system will equal the heat flow out, and temperatures at each point inside the system no longer change. At this point, transient conduction has ended, although steady-state conduction may continue if the heat flow continues [Lienhard IV and Lienhard V, 2010]. This definition describes the process of CBC-cooling in a good manner and is therefore applied to the CFD model.

In the cases presented in this thesis, steady-state is not reached during the time of CBC-cooling. After the CBC-cooling the fish is placed in an EPS-box where it is stored for approximately one hour. During this storage period the system reaches conditions which are very close to steady state where the fish temperature is almost uniform. Temperature close to the fish center continues to get lower during the storage because the skin is so cold that it keeps extracting heat from inside the fish until it reaches equilibrium. This process might take up to two hours of storage time.

2.3.7 Thermal contact resistance

The actual temperature profile through two materials in contact results in a temperature drop between the bodies. The temperature drop in the contact plane between the two materials is said to be the result of *thermal contact resistance*.

No real surface is perfectly smooth, and the actual surface roughness is believed to play a central role in determining the contact resistance. Two factors are of most importance when examining heat transfer at the joints: a) The solid-to-solid conduction at the spots of contact, and b) The conduction through entrapped gases in the void spaces created by the contact. Factor b) is assumed to represent the major resistance to heat flow, since the thermal conductivity of the gas is quite small compared to the solids [Holman, 2010].

The temperature profile between two solid materials with a thermal contact resistance is presented in Figure 2.21. Here T_1 is a temperature value inside the fish, T_3 is a temperature

value inside the belt, and point 2 is where the two bodies are in contact. The temperature values T_{2A} and T_{2B} are both positioned at the contact, representing the temperature of the two different bodies. Between these bodies is a temperature jump which is explained by the effect of the thermal contact resistance.

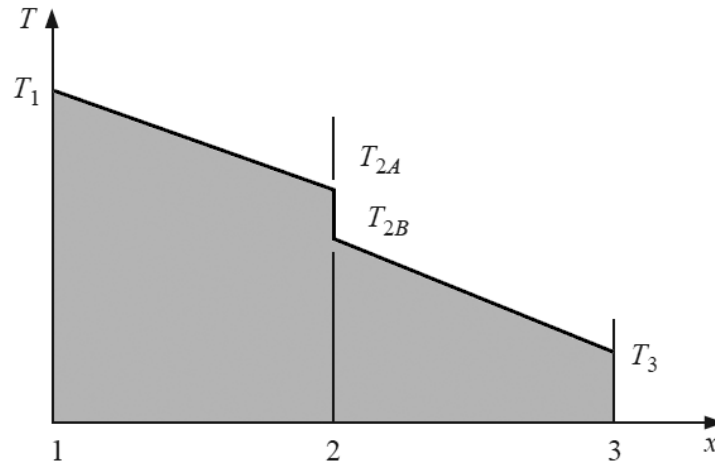


Figure 2.21: Temperature profile showing the influence of thermal contact resistance [Holman, 2010].

The two bodies in contact are the fish and the aluminium belt. When the bodies are modelled in the CFD model, the contact between them is defined as perfectly smooth. To approximate real life conditions a thin layer of contact material with very low constant thermal conductivity, $k = 0.001 \text{ W/(m K)}$, is defined and located between the two bodies in the CFD model. The thermal resistance, R , is defined as:

$$R = \frac{\Delta x}{k} \quad (2.3.12)$$

where Δx , the thickness of the contact material, is the parameter which is adjusted to get the appropriate value of R . For example, to obtain a value of $R = 0.050 \text{ m}^2 \text{ K/W}$ the thickness is set to $\Delta x = 0.05 \text{ mm}$.

2.3.8 Near wall treatment

When simulating a model which contains turbulent flows, special mesh treatment is needed where the fluid is in presence of walls. In the near-wall region the solution variables have large gradients which require careful modelling. The modelling of this region has a strong influence on the numerical solution, since walls are the main source of turbulence and vorticity formation.

The near-wall region can be divided into three layers. In the viscous sublayer (see Figure 2.22) the flow is almost laminar, and the momentum and heat transfer are mainly influenced by the molecular viscosity of the fluid. The fully-turbulent layer is mostly influenced by turbulence. Between the viscous sublayer and the fully-turbulent layer is the buffer layer where the effects of molecular viscosity and turbulence are equally important.

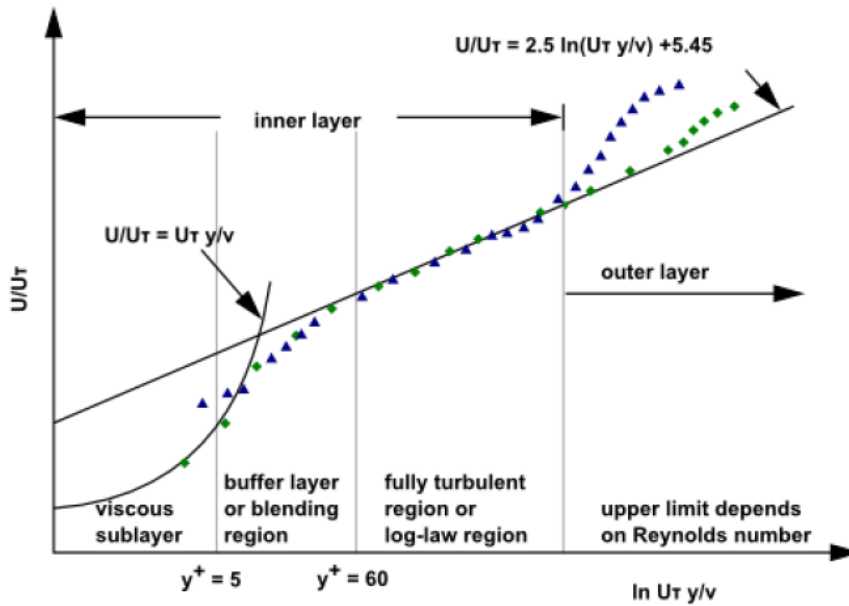


Figure 2.22: Subdivisions of the near-wall region in semi-log coordinates, with respect to y^+ [ANSYS, 2009, p. 120].

The dimensionless parameter y^+ is the distance from the wall surface to the first data point in the fluid mesh and is used to determine the type of layer in the near-wall region. This parameter can be defined as follows:

$$y^+ = \frac{y u^*}{\nu_w} \quad (2.3.13)$$

where u^* (m/s) is the friction velocity at the nearest wall, y (m) is the distance from the data point to the nearest wall and ν_w (m^2/s) is the local kinematic viscosity of the fluid [ANSYS, 2009, p. 120].

2.3.9 Error estimation

The root mean square function is used to estimate the amount of deviation between the CFD- and measured results. The function is defined as:

$$RMS = \sqrt{\left(\frac{1}{N} \sum_i^N (T_{CFD} - T_{EXP})^2\right)} \quad (2.3.14)$$

where T_{CFD} and T_{EXP} are the calculated and experimental temperature values at each measured point, respectively [Weisstein [2012]].

This chapter presents and compares the results from measurements and the CFD-models. A turbulence model is selected for the air flow and the thermal contact resistance between fish and aluminium belt is determined. The selected turbulence model and the thermal contact resistance are then applied for different cases, involving longer periods of CBC-cooling including storage and a 3D case.

3.1 Experimental results

Measurements are conducted for four different tests where the temperature settings inside the CBC-cooler is altered. The applied settings, presented in Table 3.1, are the ideal settings but the measured settings, which are used in the CFD model were obtained by measurements. The table also shows the chilling periods inside the CBC-cooler for each test. Test 4 consists twice of chilling periods of 15 and 30 minutes which is because the measurements are made for fish with different masses. Test 1 and Test 3 with chilling periods of 6 and 14 minutes, respectively, are used for comparison in this thesis. The experimental results which are not shown in this section are presented in Appendix A.

Table 3.1: Applied temperature settings and chilling periods inside the CBC-cooler for the four different measurements.

Test no.	1	2	3	4
T_{∞} [°C]	-7.4	-13.0	-14.1	-13.6
Chilling period [min]	6	10, 15, 20, 25	8, 14, 18	15, 30, 15, 30, 0

Dimensions of the two fish specimen used for later comparison are presented in Table 3.2. The lengths L and L' represent the total length and the length without head and tail as is shown in Figure 2.4.

Table 3.2: Dimensions of the fish specimen which are used for comparison for the two different temperature conditions in the CBC-cooler.

CBC settings	L [cm]	L' [cm]	m [kg]
Conventional	75	44	2.53
Modified	72	40	2.77

3.1.1 Conventional CBC-cooler settings (Test 1)

The settings used for the first case are the same as for conventional CBC-cooling of fish fillets, and are presented in Table 3.3.

Table 3.3: Conventional settings in the CBC-cooler along with the fish initial temperature.

u_{∞} [m/s]	T_{∞} [°C]	T_0 [°C]
2.6	-7.4	4.3

The fish is cooled for a period of 6 minutes in the CBC-cooler. The temperature profile inside the fish flesh during the CBC-cooling and a storage period of approximately 60 minutes is presented in Figure 3.1. As shown in the figure, the fish is chilled down to a temperature close to 2°C which is quite far from freezing. The ideal temperature for the fish after CBC-cooling should be just below the initial freezing temperature of $T_{f,i} = -0.91$ °C, as discussed earlier. Thus the temperature settings and the cooling period are changed, as shown in Section 3.1.2.

It is clear, from Figure 3.1 (at $t = 0$ min), that the initial temperature of the fish flesh is not uniform. The initial temperature, T_0 , in Table 3.3 is a selected value in the range of the measured temperatures at the three positions.

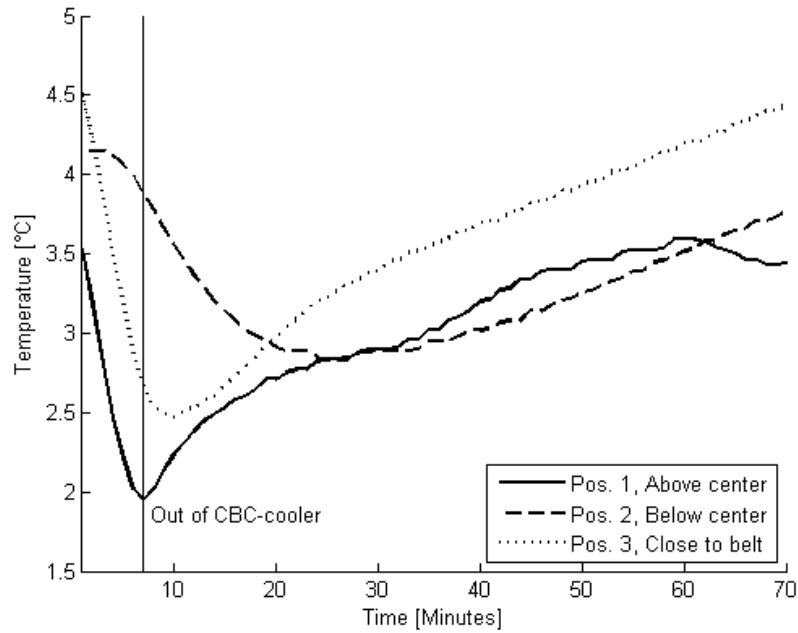


Figure 3.1: Temperature in cross section C for a period of 6 minutes with storage, for $T_{\infty} = -7.4^{\circ}\text{C}$. Vertical line indicates when the fish is put in and taken out of the CBC-cooler.

3.1.2 Modified CBC-settings (Test 3)

Since no temperatures below 0°C were monitored with the data loggers when using the conventional CBC-cooler settings, different settings are applied. The settings used for this case are presented in Table 3.4.

Table 3.4: Modified settings in the CBC-cooler along with the fish initial temperature.

u_{∞} [m/s]	T_{∞} [$^{\circ}\text{C}$]	T_0 [$^{\circ}\text{C}$]
2.7	-14.1	4.1

These settings are applied for three different chilling time periods: 8, 14 and 18 minutes. The results for each of those periods are compared in Figure 3.2. The figure shows that after storing the fish for over an hour the temperature inside the fish flesh is almost uniform. This does not apply for position 1 for the 8 minute CBC-cooling, which might indicate errors in the data logger during measurements at that position.

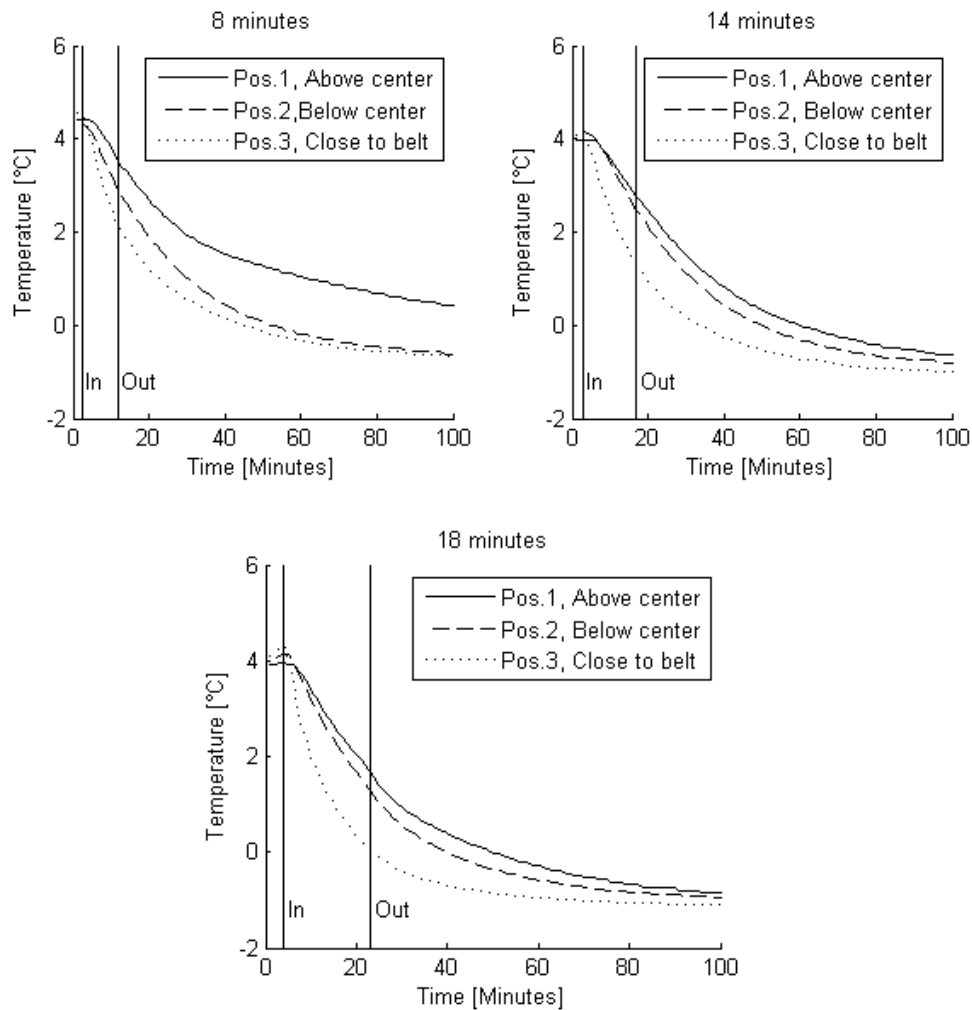


Figure 3.2: Temperature in cross section C for different time periods, with storage, for $T_{\infty} = -14.1^{\circ}\text{C}$. The vertical line indicates when the fish is taken out of the CBC-cooler.

Table 3.5 presents the temperature inside the fish 80 minutes after the start of CBC-cooling. The table shows that CBC-cooling for 8 minutes results in temperatures below zero for positions 2 and 3, but above zero for position 1. The temperature decreases further when the time inside the CBC-cooler is increased, as expected. Since the difference in temperature decrease between the 14-minute and the 18-minute case is not severe, and in both cases the temperatures reach values below zero, the 14-minute case is selected for comparison. In addition, the computational time for the 14-minute case is much shorter than for the 18-minute case which is important to think of when working with CFD.

Table 3.5: Temperature inside the fish 80 minutes after the start of CBC-cooling for three different time values in cross section C.

Time [min]	Pos. 1	Pos. 2	Pos. 3
8	0.68	-0.45	-0.56
14	-0.41	-0.65	-0.91
18	-0.66	-0.83	-1.07

The temperature measured inside cross section A is shown in Figure 3.3 for the same chilling periods as presented before (8, 14 and 18 minutes). Since cross section A is relatively smaller than cross section C, only two data loggers are inserted for temperature measurements, at positions 1 and 2. It is interesting to see how the temperature behaves at position 2 for CBC-cooling for 14 and 18 minutes. The temperature profile of the 18-minute cooling in Figure 3.3 shows the change in a more clear way, i.e. immediately after the fish is taken out of the CBC-cooler the temperature below center, which then has reached a value of -2.5°C , has a quick rise. This is because after the fish is released from its contact with the aluminium belt, the bottom surface extracts thermal energy from inside the fish until it reaches equilibrium resulting in a uniform temperature.

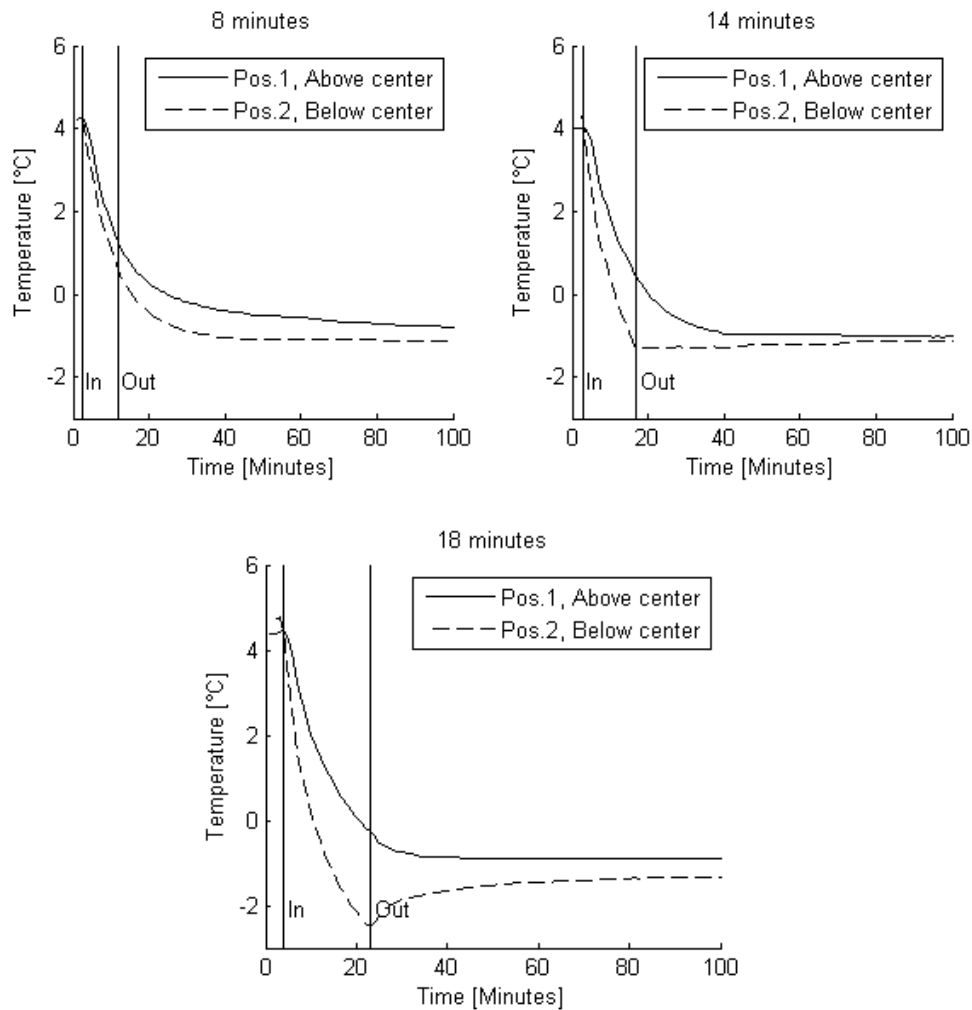


Figure 3.3: Temperature in cross section A for different time periods, with storage for $T_{\infty} = -14.1^{\circ}\text{C}$ inside CBC-cooler. Vertical lines indicate when the fish is put in and taken out of the CBC-cooler.

The temperature inside cross section A after 80 minutes, including CBC-cooling, is presented in Table 3.6. It is interesting that the temperature decrease does not vary much between the three holding times. This might be caused by the amount of fish flesh in cross section A being significantly lower than in cross section C, which causes less heat to be stored.

Table 3.6: Temperature ($^{\circ}\text{C}$) inside the fish 80 minutes after the start of CBC-cooling for three different time values in cross section A.

Time [min]	Pos. 1	Pos. 2
8	-0.72	-1.11
14	-1.01	-1.14
18	-0.91	-1.37

The reason why a numerical model is created for cross section *C* instead of *A* is because cross section *C* is positioned at the loin part of the fish, which includes a higher amount of fish flesh and therefore needs closer temperature inspection. Since the amount of flesh is highest in cross section *C* the model should capture the thermal properties, described in Section 2.1, in a more precise manner.

It is clear from the results presented above that lower temperatures are to be expected in the thin tail part (cross section *A*) as compared to the thicker loin part (cross section *C*). To protect the tails from excessive freezing, the cooling parameters must be chosen so that the applied cooling is lesser than optimal for the loin part. The results in Tables 3.5 and 3.6 show that the suggested cooling time for fish weighing 2-3 kg and $T_{\infty} = -14.1^{\circ}\text{C}$ is 15 to 20 minutes. By choosing an air temperature of -14°C instead of -25°C to -20°C , lesser temperature gradients should be obtained in each fish, therefore securing more even product quality.

3.2 Numerical results and comparison

In this section a CFD model is adopted to match the results obtained from experiments, which were conducted when the fish is CBC-cooled for periods of 6 and 14 minutes. Most of the results are obtained by using the two dimensional model described in Section 2.3.1. The thermal contact resistance and the turbulence model is determined by comparison with Test 1. Those settings are then used to compare with Test 3, which includes CBC-cooling for 14 minutes and a storage period of 60 minutes. A 3D model is generated to compare with Test 3. Finally a simulation of a CBC-cooling period of 30 minutes and storage for one hour is applied to study the temperature behaviour and if freezing occurs in the flesh.

3.2.1 Conventional CBC-cooler settings

When running a CFD-simulation it is very important to generate a model which converges both in time and space. To estimate if the model converges in space is, in this case, to increase the height of the control volume until it no longer affects the temperature at position 1. When deciding the height of the computational domain, three heights were

tested: 150 mm, 200 mm and 250 mm. The results obtained with these different heights show that there is a difference in the solution between 150 mm and 200 mm but no difference between 200 mm and 250 mm. The height of the computational domain is therefore set to 200 mm. Time convergence is obtained by adjusting the time step size so that the Courant number (see Section 2.3.4) is satisfactory.

The settings in the CBC-cooler used for this comparison are as described in Section 3.1.1. For these settings the temperature inside the fish does not reach a value below 2°C, as shown in Section 3.1.1. As shown in Table 2.1 no significant changes occur with regards to the thermal fish properties until below 0°C. The measured temperature in the fish flesh is not completely uniform and has an initial temperature ranging from 3.7°C to 4.6°C. For this comparison the initial temperature from *FLUENT* and measurements are given the same value for the best comparison.

Thermal contact resistance

As mentioned in Section 2.2, three temperature data loggers, which were inserted in cross section *C* two below center and one above (See Figure 2.5), are used for comparison. The thermal contact resistance, discussed in Section 2.3.7, is highly influential on the temperature measured by the data loggers below center. Similarly the temperature above the center of the fish is mainly influenced with which turbulence model is used.

In research done by Margeirsson et al. [2011] a value of $R = 0.050 \text{ m}^2 \text{ K/W}$ was adopted for thermal contact resistance between fish fillets and food packaging. The value of R could be as high as $0.2 \text{ m}^2 \text{ K/W}$ but since the water content of fresh cod is as high as 80 – 82%, a lower value of R may be expected. In this previously mentioned research a value of $R = 0.050 \text{ m}^2 \text{ K/W}$ yielded a good agreement between experimental and simulated results and will therefore be examined in this study. The value of R for cod fish is a very delicate parameter which needs adjustment for different settings. Results obtained with values ranging from $R = 0.025 \text{ m}^2 \text{ K/W}$ to $R = 0.050 \text{ m}^2 \text{ K/W}$ is introduced and compared with measurements.

In this section the temperatures below the center of the fish are compared to decide what value of R is to be selected. Figures 3.4 and 3.5 give a visual comparison between the experimental and calculated results for different values of R . A numerical comparison is presented in Table 3.7 where the root mean square (RMS) error between measurements and simulated results is compared for the different values of R . Note that the temperature scales for Figures 3.4 and 3.5 range from 3.95 to 4.2°C and 2.6 to 4.6°C, respectively.

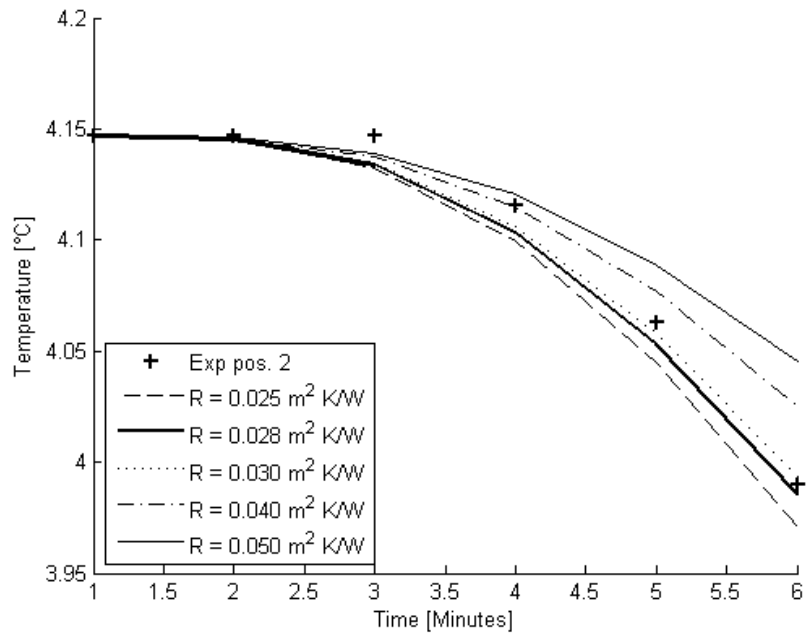


Figure 3.4: Temperature comparison 16 mm above belt for different values of R .

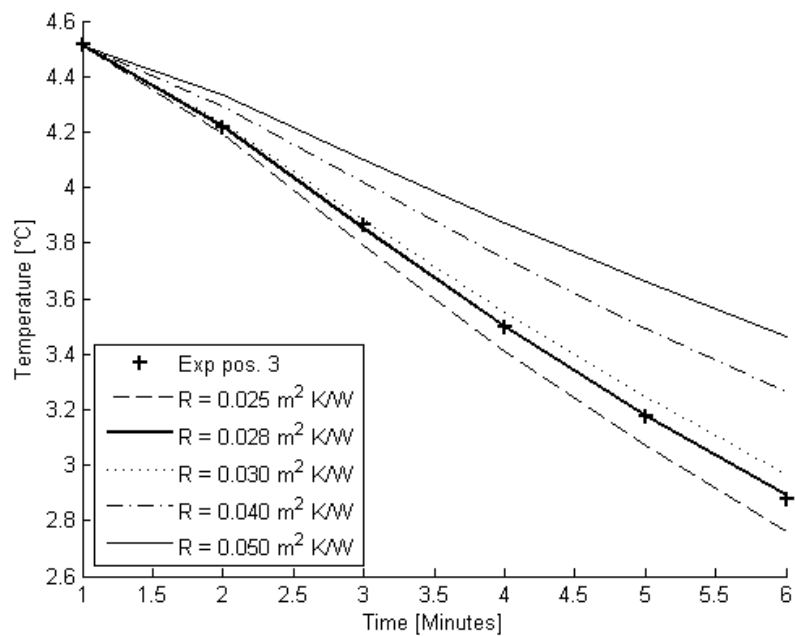


Figure 3.5: Temperature comparison 6 mm above belt for different values of R .

The results presented in Table 3.7, along with the visual comparison in Figures 3.4 and 3.5, show that the measured values are in almost every case positioned in between $R = 0.025 \text{ m}^2 \text{ K/W}$ and $R = 0.030 \text{ m}^2 \text{ K/W}$. It is therefore assumed that a value between these two, closer to $R = 0.030 \text{ m}^2 \text{ K/W}$, is ideal for this case. Further examination shows that $R = 0.028 \text{ m}^2 \text{ K/W}$ gives the best results and is therefore selected as the value for the thermal contact resistance.

Table 3.7: RMS error comparison ($^{\circ}\text{C}$) for different values of R , positioned 6 mm and 16 mm above the belt.

$R \text{ [m}^2\text{K/W]}$	Pos. 2 (16 mm)	Pos.3 (6 mm)
0.050	0.03	0.36
0.040	0.02	0.24
0.030	0.01	0.05
0.028	0.01	0.01
0.025	0.01	0.08

Turbulence model

Since the air flow around the fish surface is considered turbulent a turbulence model needs to be selected to simulate the air flow. It was decided to implement three different turbulence models: $k - \epsilon$ Realizable, $k - \epsilon$ RNG and $k - \omega$ SST [ANSYS, 2009, p. 51-72]. The results from these models are compared and the model which gives the best results is selected for further calculations. Mesh 1, defined in Section 2.3.2, is used for this comparison, since it required less computational cost than the other meshes. As mentioned before, the forced convection, produced by air flow, impacts the temperature change greatly at position 1. It is therefore important to select a turbulence model which gives acceptable results. Results obtained from the different models are compared numerically in Table 3.8 and visually in Figure 3.6.

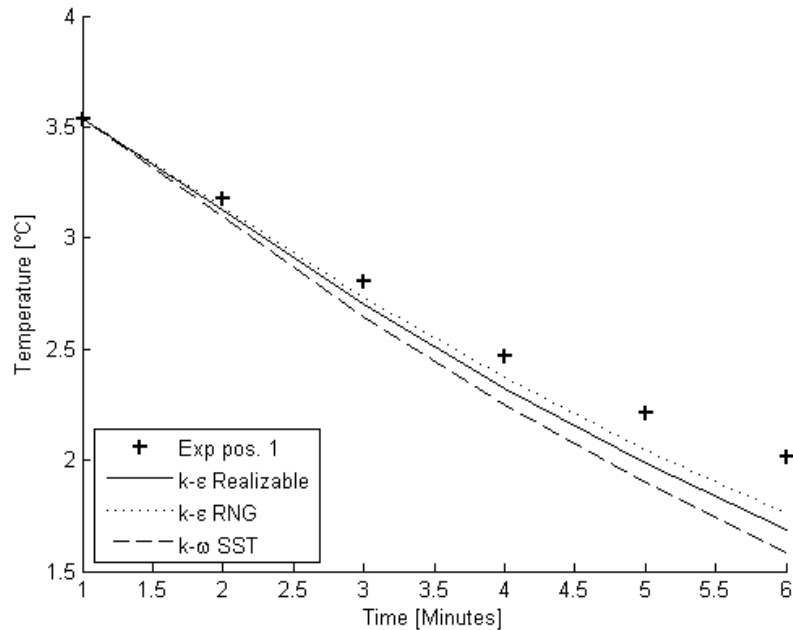


Figure 3.6: Temperature comparison 56 mm above belt for different turbulence models

The results presented in Figure 3.6 and Table 3.8 show that the $k - \varepsilon$ RNG turbulence model gives the best comparison. The $k - \varepsilon$ RNG turbulence model is therefore used for further calculations.

Table 3.8: RMS error comparison ($^{\circ}\text{C}$) for different turbulence models positioned 56 mm above belt.

Turbulence model	Pos. 1 (56 mm)
$k - \varepsilon$ Realizable	0.18
$k - \varepsilon$ RNG	0.14
$k - \omega$ SST	0.25

3.2.2 Mesh refinement

The selected R -value and turbulence model are now applied to Mesh 2, to see if it yields more accurate results. The results for the two meshes are compared in Table 3.9. The highest percentage difference is approximately 44% at position 2 (16 mm above belt). Since this is only an increase from a RMS error of 0.009°C to 0.005°C , which is very small, no further mesh refinement is applied for this case. The highest RMS error, at position 1 (45 mm above belt), might be explained by the fact that these results are for a

2D case where the fish thickness is uniform and not a full 3D case where the thickness varies along the fish length.

Table 3.9: RMS error ($^{\circ}\text{C}$) comparison of Mesh 1 and Mesh 2.

Pos. no.	Dist. from belt [mm]	Mesh 1	Mesh 2
1	56	0.136	0.127
2	16	0.009	0.005
3	6	0.007	0.006

A comparison of the y_{\max}^+ values for Meshes 1 and 2 is presented in Table 3.10. The comparison shows that when the cell size is reduced by 50% the value of y^+ is reduced by approximately the same amount. Both values of y_{\max}^+ are in the buffer layer region as presented in Section 2.3.8.

Table 3.10: Comparison of y_{\max}^+ values at the fish surface, adjacent to the air, for the two meshes.

	Mesh 1	Mesh 2
y_{\max}^+	20.46	10.80

The temperature distribution within the computational domain, for Mesh 2, is presented in Figure 3.7, where the cold air is blasted from the right side. The figure shows that the temperature gradient from the fish surface is almost the same as from the fish bottom, towards the fish center. This indicates that the effect of forced convection cooling is almost equivalent to that of contact cooling.

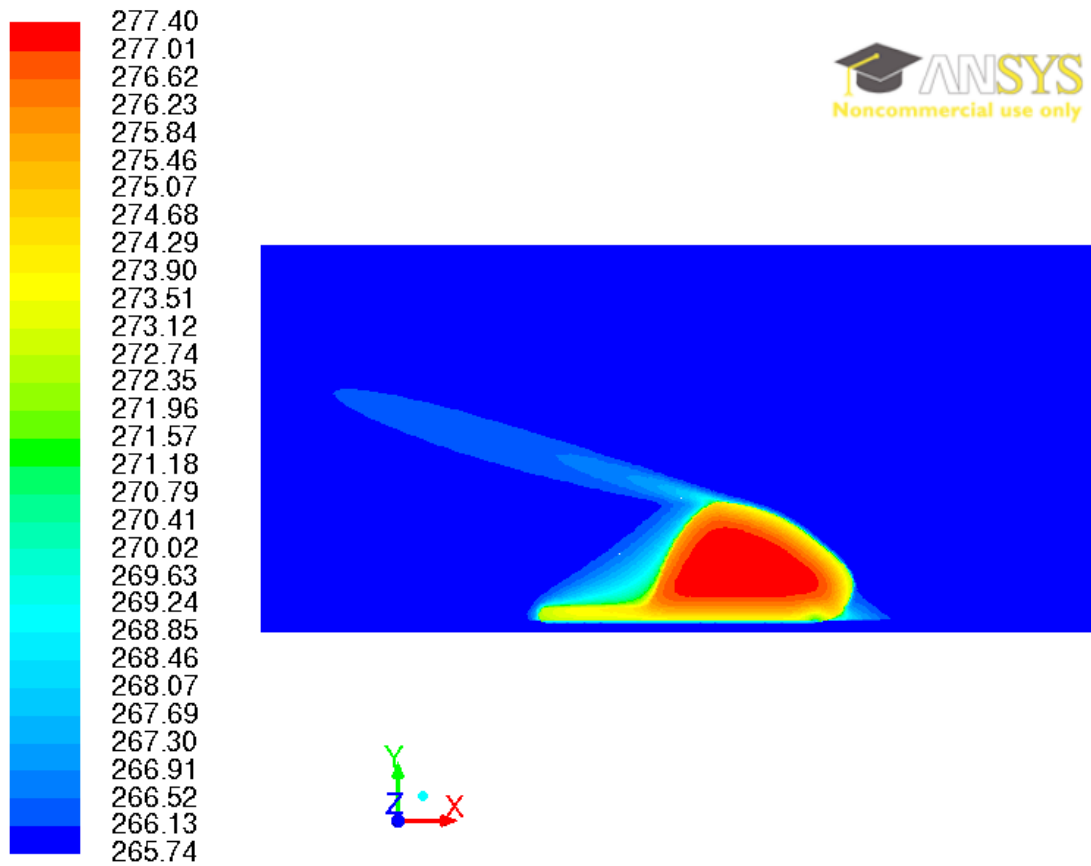


Figure 3.7: Temperature (K) distribution after 6 minutes in the CBC-cooler.

To get a better idea of the amount of heat extracted from the fish, Figure 3.8 shows a comparison between the contact and air cooling by using Mesh 2. The figure compares a vertex average of the heat flux extracted from the fish. Heat extraction is a negative value but is presented as an absolute value in Figure 3.8. The figure shows that the amount of heat extracted from the fish bottom, through contact, is approximately 30 to 55 W/m^2 higher than from the fish surface in contact with air, at each time. The belt and air combined are both very important factors for this setup, although the effect of the belt is higher.

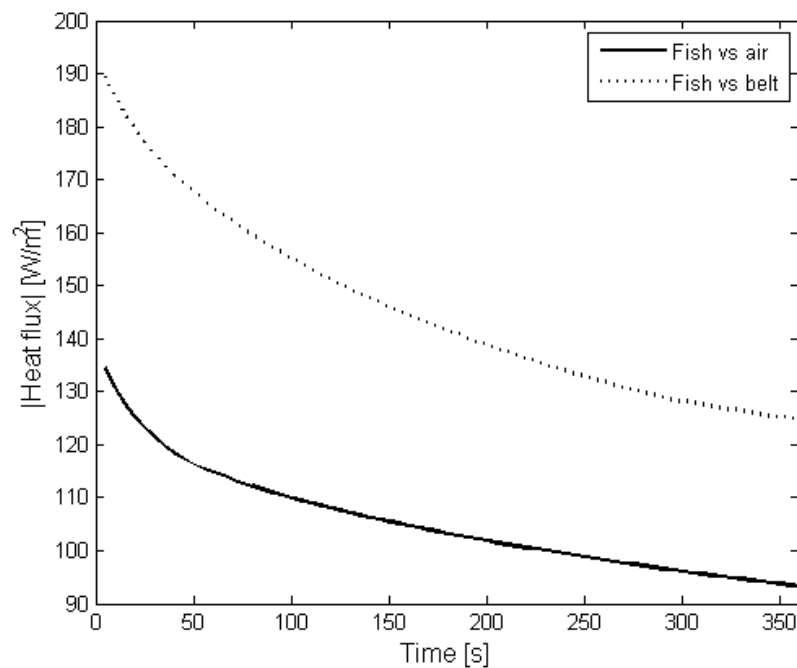


Figure 3.8: Heat flux (W/m^2) through the fish bottom and top.

Velocity profile

The air velocity profile within the computational domain, after 6 minutes of CBC-cooling, is presented in Figure 3.9. The geometry of the fish causes the air velocity to increase when the air travels over the cross section. Magnitude of the air velocity is highest close to the top of the fish with a value of 4.0 m/s which is higher than the inlet velocity of 2.6 m/s . The position of the highest velocity should indicate where the effect of forced convection is highest.

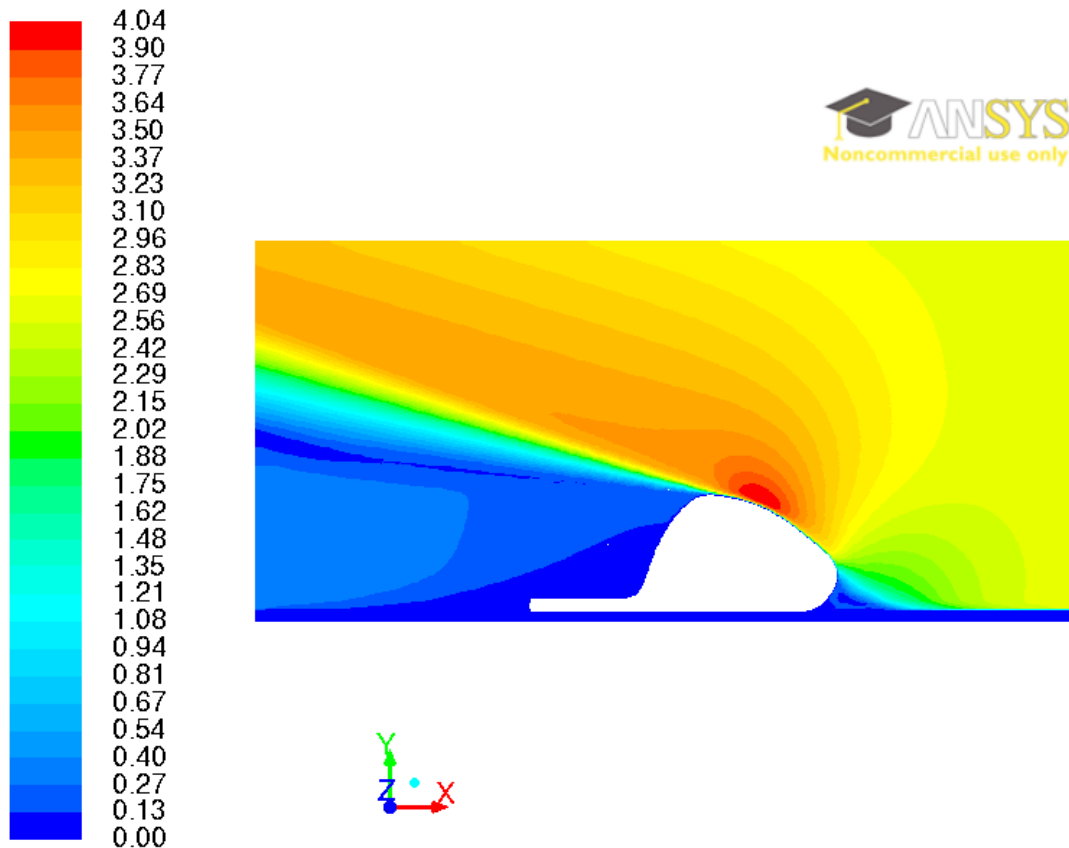


Figure 3.9: The velocity magnitude (m/s) distribution within the computational domain.

3.2.3 Extended CBC-cooling with storage

In this section the model is expanded so that the results include a storage period of one hour. The turbulence model and thermal contact resistance, presented in Section 3.2.1 are implemented for this case. A comparison is made with experimental results from Test 3, when the CBC-cooler is set to $T_{\infty} = -14.1^{\circ}\text{C}$ and the fish is cooled for a period of 14 minutes. After the CBC-cooling the fish is placed in an EPS-box and stored for over an hour. Measurements show that when the fish is placed in EPS boxes, the measured flesh temperature has not reached the initial freezing temperature. During a storage period of one hour the flesh temperature equalises and the measured temperature reaches an almost uniform value close to -0.5°C .

Immediately after the CBC-cooling, the air flow is reduced to 0 m/s. Presented in Figure 3.10 is the velocity profile in the computational domain just after the air velocity has been reduced. The flow looks realistic since it shows a reduction in velocity and no strange behaviour. The circular motions on both sides are explained by the fact that the

fluid particles which were at 2.7 m/s when the boundary conditions were changed are adjusting in the domain.

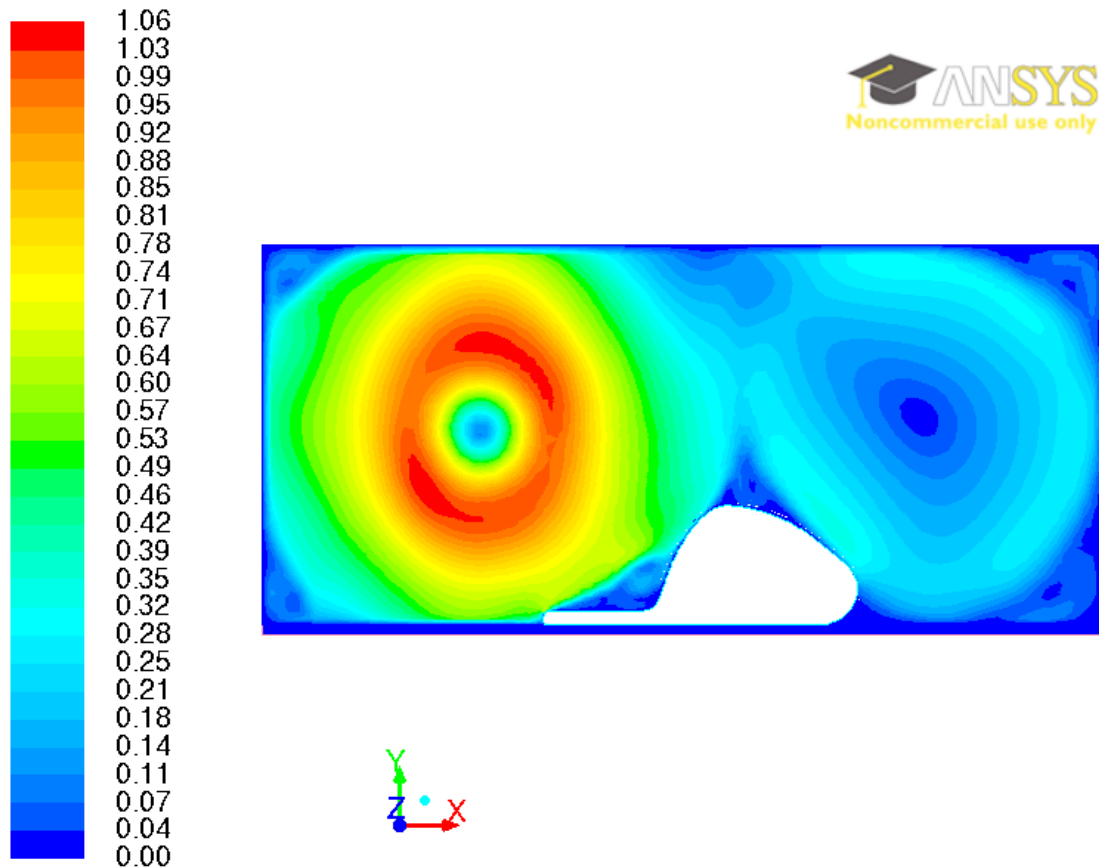


Figure 3.10: Velocity (m/s) in the computational domain immediately after the CBC-cooling.

Since this case includes longer CBC-cooling and a storage period of one hour, Mesh 3, which includes a more refined mesh at the fish surface, is introduced and compared with measurements. Mesh 3 was not used for the conventional settings because that case was used to select the turbulence model and the thermal contact resistance, which needed no further mesh refinement.

The results obtained with Meshes 1, 2 and 3 are compared with experimental results in Table 3.11. These results show a good comparison but not as good as for the 6-minute case (see Section 3.2.2). It is clear that the surface refinement of Mesh 3 has a great influence on the results with the highest impact on position 1 (45 mm above belt), where the error is reduced by 0.2°C.

Table 3.11: *RMS error ($^{\circ}\text{C}$) comparison for the three different meshes after CBC-cooling and storage for one hour.*

Pos. no.	Dist. from belt [mm]	Mesh 1	Mesh 2	Mesh 3
1	45	0.35	0.38	0.19
2	13	0.24	0.20	0.18
3	8	0.37	0.33	0.32

The calculated results are compared visually with measurements in Figure 3.11 for Mesh 3. The figure shows that the temperature profiles follow each other almost perfectly during the CBC-cooling. After that the model predicts higher temperatures which might be explained by inaccurate modelling of the boundary conditions during the storage period.

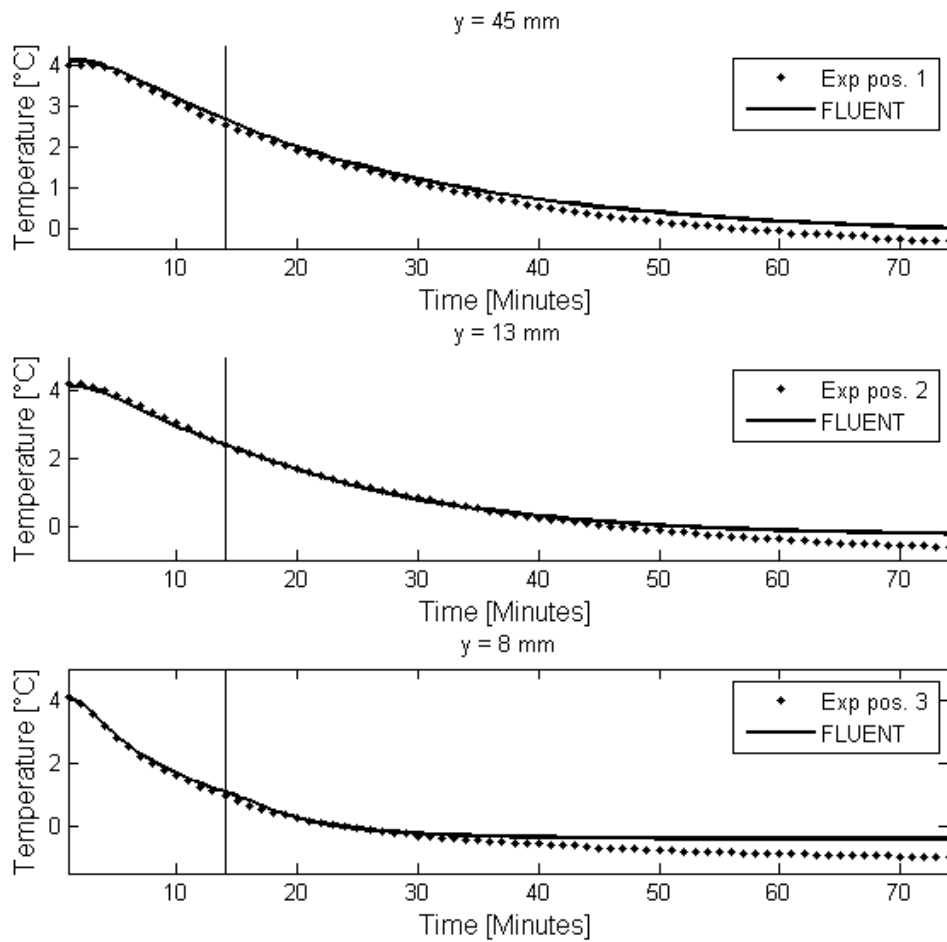


Figure 3.11: Results from *FLUENT* compared with experimental results during CBC-cooling and for one hour of storage.

A further comparison is presented in Table 3.12 where the temperatures from *FLUENT*, with Mesh 3, and measurements are compared after 14 minutes of CBC-cooling and one hour of storage. The results are in good agreement with measurements for all points, though an overestimation of the temperature in the results from *FLUENT* is clear. Since the measured temperature is located at the part of the fish where it is thickest, this overestimation might be because the thickness is considered uniform and therefore no 3D effects are considered.

Table 3.12: Temperature comparison after CBC-cooling and one hour of storage. All values are in °C.

Time [min]	Pos. 1 (45 mm)	Pos. 2 (13 mm)	Pos. 3 (8 mm)
Experimental	-0.41	-0.65	-0.91
<i>FLUENT</i>	0.00	-0.22	-0.40
Difference	0.41	0.43	0.51

The temperature distribution within the computational domain, from the end of the CBC-cooling until the end of a storage time of one hour, is presented in Figure 3.12. The figure shows that the fish has not reached a completely uniform temperature after one hour. The temperature is highest at the upper left part of the fish which might be explained by the fact that the air is blasted at the right side of the fish during the CBC-cooling resulting in lower temperatures in that area. The figure also shows that during a storage period of one hour the temperature inside the fish has almost reached a uniform temperature. For a completely uniform temperature in the flesh, it is assumed that a longer storage period is required.

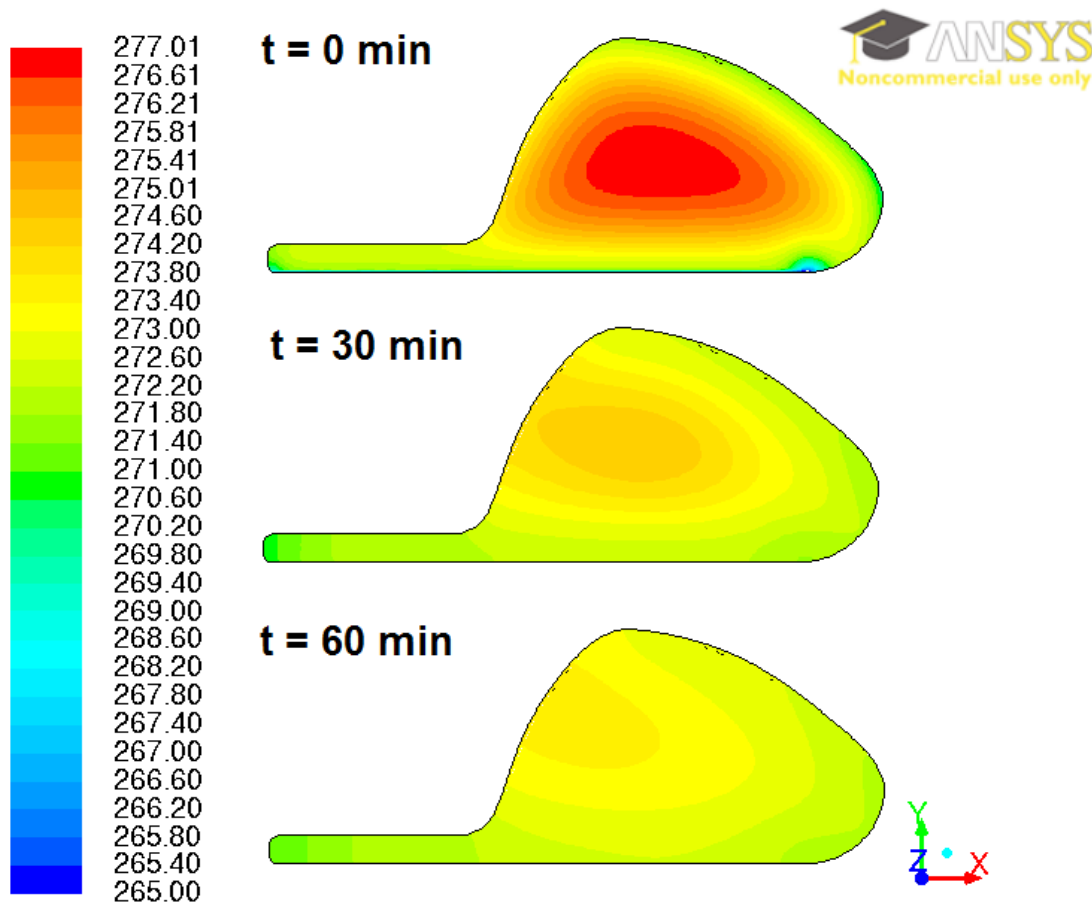


Figure 3.12: Temperature distribution (K) in the computational domain from the end of CBC-cooling to a storage time of one hour.

The y_{max}^+ values at the fish surface are compared for the three meshes in Table 3.13. All the y_{max}^+ values are positioned in the buffer layer region, although Mesh 3 is very close to the viscous boundary layer (see Figure 2.22). The fact that the y_{max}^+ value for Mesh 3 is almost at the intersection between the viscous boundary layer and the buffer layer might explain the better results, which are obtained with that mesh.

Table 3.13: Comparison of y^+ values for the three meshes.

	Mesh 1	Mesh 2	Mesh 3
y_{max}^+	21.16	11.06	6.59

The heat flux through the fish surface, in contact with air, is highly affected by the grid size at the fish surface. The grid dependency is clear in Figure 3.13 which shows that the

heat flux increases with a more refined grid at the surface. This shows that there is a lot of activity in the region very close to the surface which can be captured with a sufficiently refined mesh. Note that the values presented in Figure 3.13 are absolute.

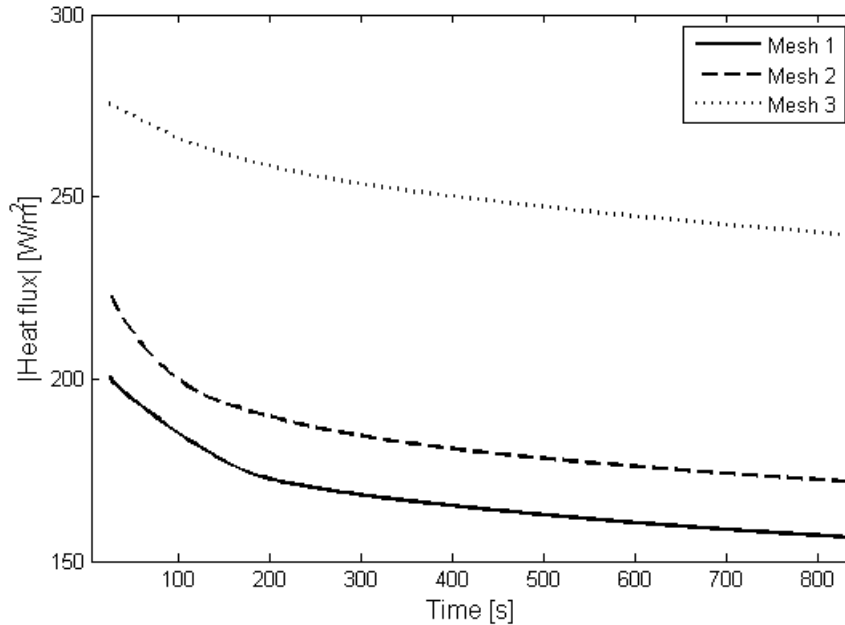


Figure 3.13: Comparison of heat flux (W/m^2) in terms of the three meshes, caused by air blasting.

3.2.4 3D results

The solution for the 3D model is compared with measurements for the CBC-cooling and a storage period of one hour in Table 3.14 and Figure 3.14. The calculated results show a very good comparison with measurements, especially for position 1 (45 mm above belt).

Table 3.14: RMS error ($^{\circ}C$) comparison between the 3D model and measurements after CBC-cooling and storage for one hour.

Pos. no.	Dist. from belt [mm]	RMS [$^{\circ}C$]
1	45	0.09
2	13	0.28
3	8	0.35

The comparison in Figure 3.14 shows that the model predicts lower temperatures during the CBC-cooling at positions 2 and 3, but higher temperatures during the storage period. The model results at position 1 show a very good comparison during the whole process.

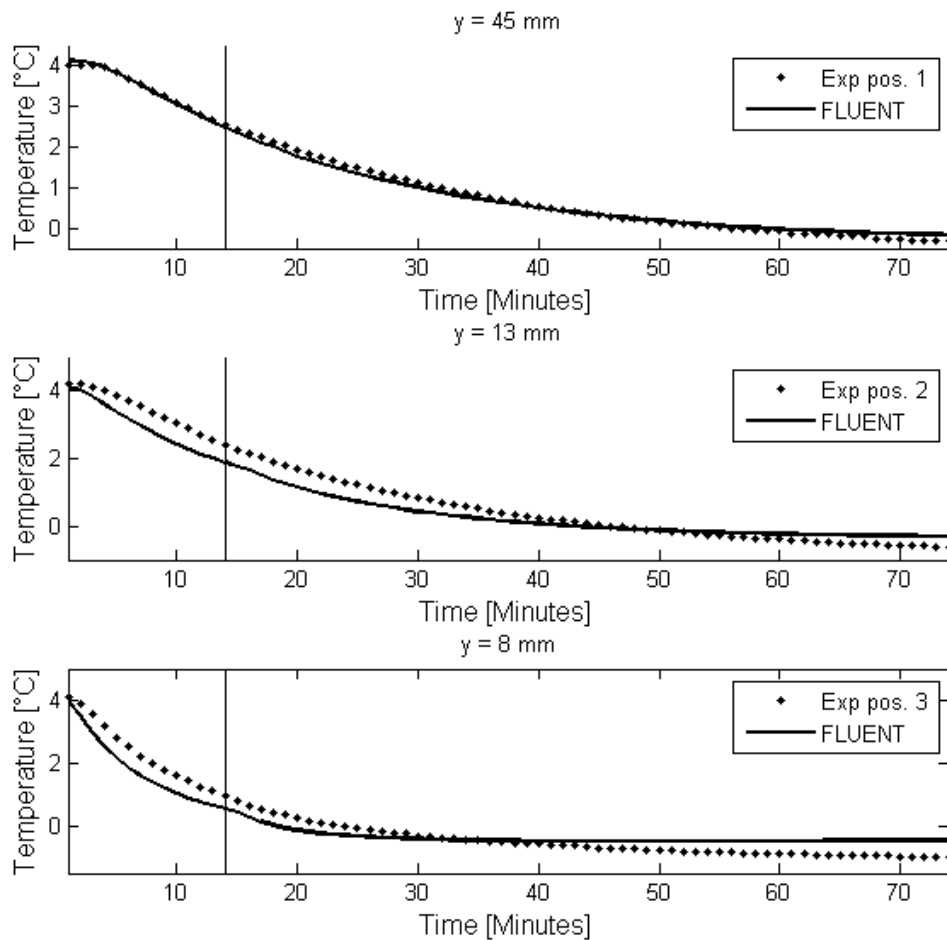


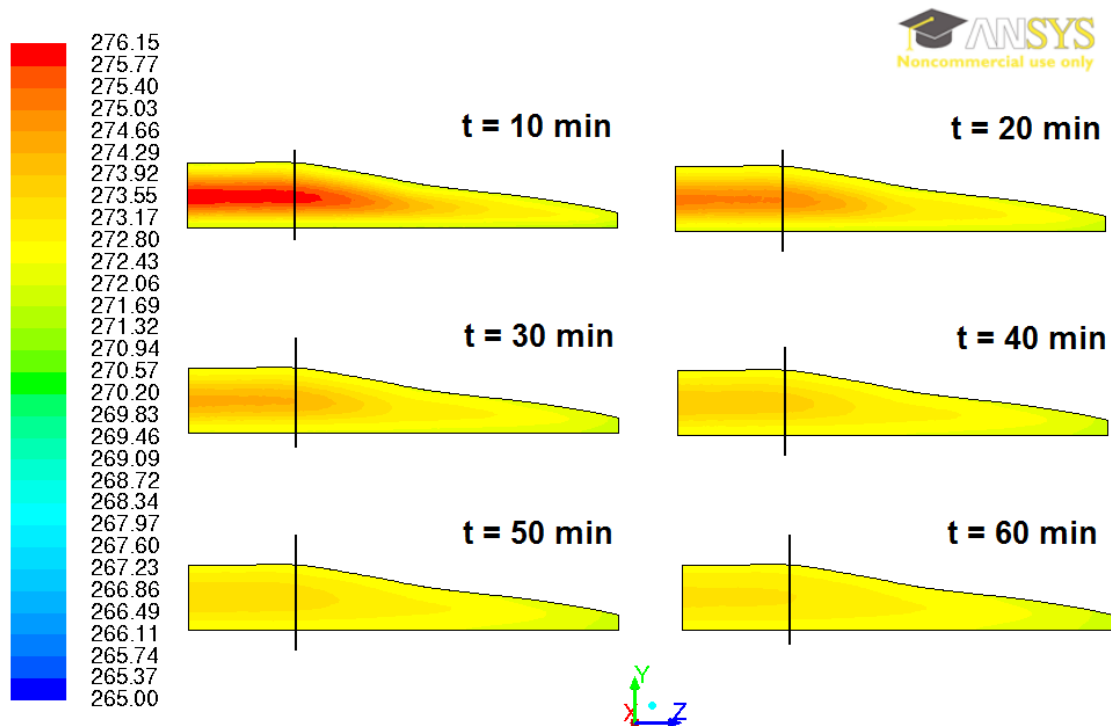
Figure 3.14: Results from the 3D case in FLUENT compared with measured results during the CBC-cooling and for one hour in storage.

The temperatures after 14 minutes of CBC-cooling and one hour of storage are compared in Table 3.15. The difference between calculated and measured temperatures are also compared to see how close the model solution is to the measurements. The comparison shows that the difference is smallest at position 1 and largest at position 3. This might be explained by the fact that the mesh inside the fish body is more refined in 2D than in 3D, causing more accurate results in the 2D case.

Table 3.15: Temperature comparison ($^{\circ}\text{C}$) after CBC-cooling and one hour of storage.

Time [min]	Pos. 1	Pos. 2	Pos. 3
Experimental	-0.41	-0.65	-0.91
FLUENT	-0.13	-0.27	-0.42
Difference	0.28	0.38	0.49

A longitudinal cross section of the fish, positioned at the same x-coordinates as the temperature monitors (See Figures 2.5 and 2.11), is examined. The temperature distribution along the fish length, with a 10 min interval, during the storage period is shown in Figure 3.15. The vertical lines in the figure show the position of cross section C. The figure shows that the fish flesh keeps getting colder without any applied external cooling, such as air blasting. It is clear that the colder parts of the fish, closer to the tail, affect the temperature at cross section C by removing more heat from it than if the fish thickness is uniform. If the thickness of the fish is uniform, as for the 2D case, the longitudinal effect would look the same as at the left hand side of Figure 3.15, i.e. the effect would be negligible.

**Figure 3.15:** Temperature distribution (K) in the length cross section of the fish during storage.

The y_{max}^+ value at the fish surface, obtained from the CFD model, is 12.90. This value is

positioned in the buffer layer region (see Figure 2.22) and has almost the same value as Mesh 2. More accurate results might be obtained by refining the grid at the fish surface, resulting in a value of y_{max}^+ closer to the viscous sublayer, which was obtained with Mesh 3.

3.2.5 30 minute CBC-cooling

In this section a 30 minute long CBC-cooling process is simulated. Since no measurements were made to compare with these results, the results are only used to see what the model predicts and how it handles the fish thermal property changes as described in section 2.1. The temperature is monitored at the same positions as for Test 3 (see Section 3.2.3), i.e. 8, 13 and 45 mm above belt.

The predicted temperature in the fish flesh at cross section *C* is presented in Figure 3.16. The lowest value at position 3 is $T = -0.78^\circ\text{C}$ which shows that the fish flesh has not reached the initial freezing temperature of $T_{f,i} = -0.91^\circ\text{C}$.

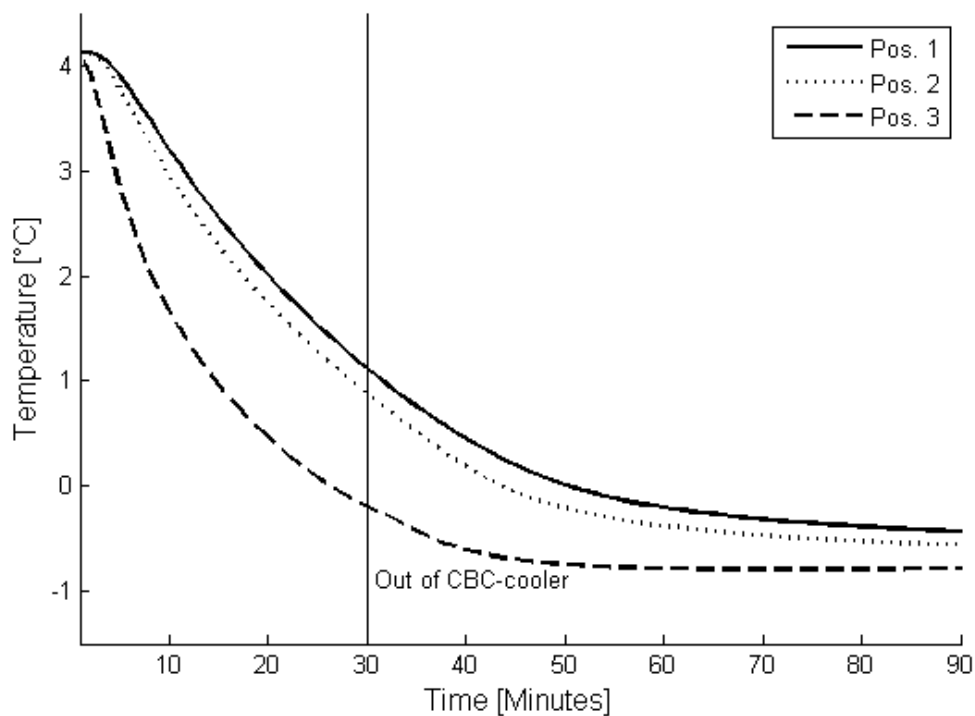


Figure 3.16: Results from the CFD model in FLUENT where 30 minutes of CBC-cooling and one hour of storage are applied.

The temperature distribution within the cross section after one hour of storage, which is

shown in Figure 3.17, indicates that the fish flesh has not reached uniform temperature. One might therefore assume that for a longer period of CBC-cooling, longer storage time is required. Figure 3.16 indicates, on the other hand, that the temperature inside the fish has almost reached a uniform temperature.

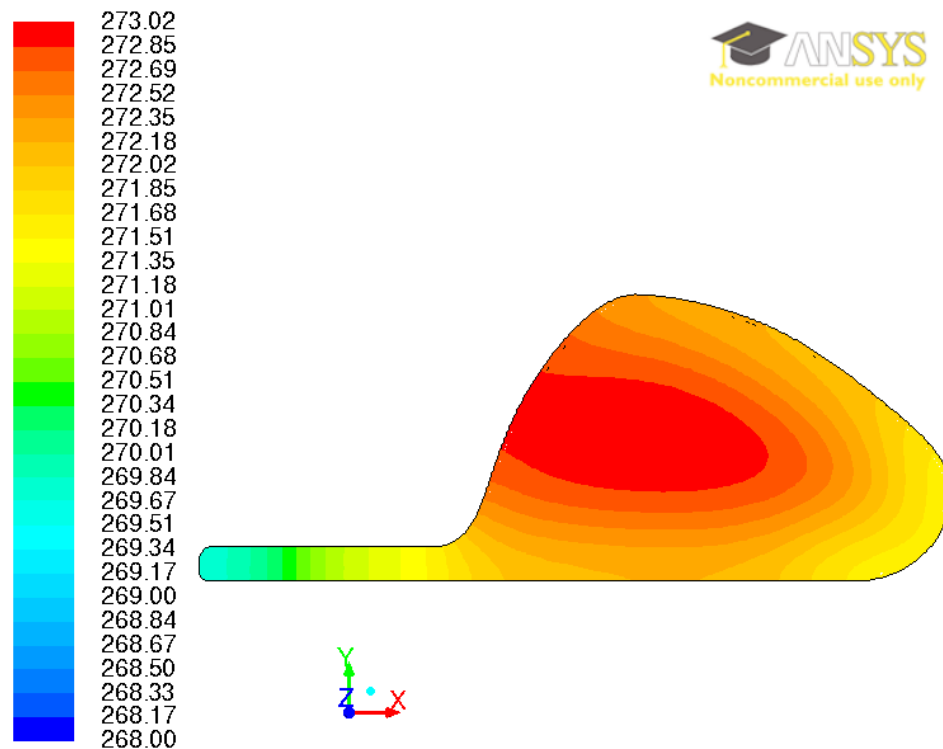


Figure 3.17: Temperature distribution (K) in cross section C after 30 minutes of CBC-cooling and storage for one hour.

3.2.6 Air flow comparison

The air flow within the computational domain, is presented for the 2D and 3D models in Figures 3.18 and 3.19, respectively. The flow in Figure 3.18, which is taken at cross section C, shows a separation close to the belt where the air hits the fish. This separation might explain the low temperature at the right side of the fish, close to belt, after the CBC-cooling (see e.g. Figure 3.12). A separation is also found at the left side of the thickest part of the fish which might be caused by its steep surface.

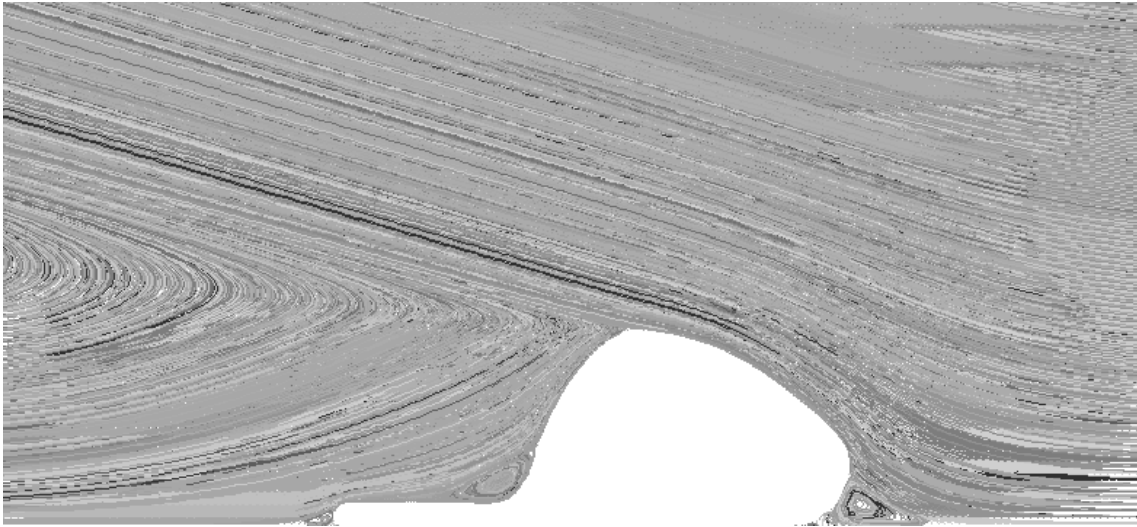


Figure 3.18: *Air flow at cross section C in 2D.*

The flow presented in Figure 3.19 is from the 3D model and is positioned at the end of the fish, closest to the head. The fish geometry is smoother at this position, hence causing less separation in the air flow than what is shown in Figure 3.18. Both figures have in common the large separation which starts to form after the air has hit the fish. If the computational domain is larger, positioning the air outlet further to the left, different behaviour of the air flow might be observed. Since this large separation is located behind the fish it is assumed that its effects are negligible to the final results.

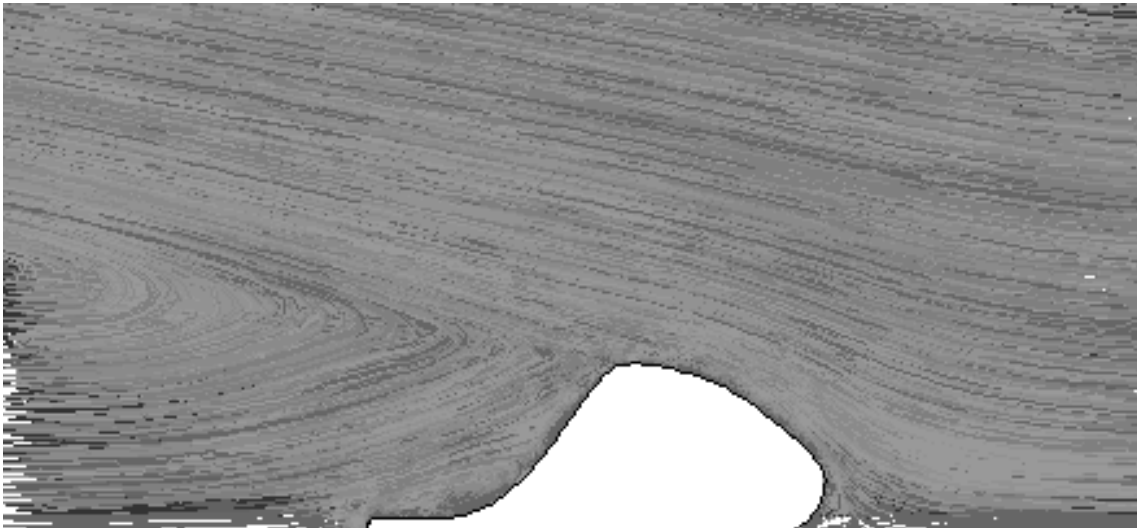


Figure 3.19: *Air flow close to the fish head in 3D.*

The flow presented in Figure 3.20 is from the 3D model and is positioned at cross section A, close to the tail. The figure shows that the large separation behind the surface, as noticed in Figures 3.18 and 3.19, is not present. This is because the height of the fish at cross section A is 32 mm compared to 63 mm at cross section C. In addition, cross section C includes steeper surfaces than cross section A. Note that the figures do not show the complete computational domain.

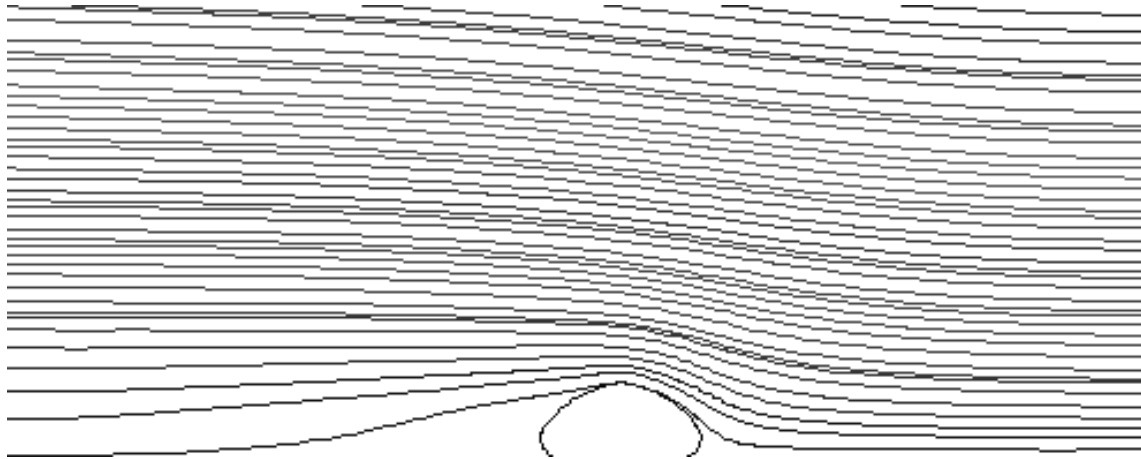


Figure 3.20: Air flow close to the fish tail in 3D.

CHAPTER 4

Conclusions

Results from the CFD simulations were generally in good agreement with the experimental results. The thermal contact resistance between the fish and aluminium belt was determined as $R = 0.028 \text{ m}^2 \text{ K/W}$ in Section 3.2.1. For the conventional CBC-cooler settings, this R value resulted in RMS errors of 0.009°C and 0.007°C at positions 2 and 3, respectively. Note that this comparison only included a chilling period of 6 minutes and no storage. The same R value was applied for the extended chilling process, including storage, in Section 3.2.3. For that process, RMS errors of 0.183°C and 0.319°C were obtained at the corresponding positions. This high increase in the error might be caused by the storage period, which was included for the second case, or that the thermal contact resistance R changes between fish samples.

The $k - \varepsilon$ RNG turbulence model was preferred over the $k - \varepsilon$ Realisable and $k - \omega$ SST models to simulate the air flow in the computational domain. The model was applied for three different meshes for the extended chilling period with storage. Mesh 3, which included a refined grid at the fish surface adjacent to the air, yielded the best results.

A simulation of the 3D model showed that the height differences along the fish effected the temperature distribution at cross section C . The results from the best 2D case (Mesh 3) and the 3D case are compared in Table 4.1. It is clear that the 2D and 3D results are not in very good agreement when compared to each other. The 3D model gives very good results for position 1 but not as good as the 2D model for positions 2 and 3. The most likely reason for this difference is, as mentioned before, the longitudinal effect of the model, i.e. the height difference along the fish length. The contact area between the fish and belt/EPS box also varies along the fish length (see Figure 2.15), which might cause this difference.

Table 4.1: RMS error ($^{\circ}\text{C}$) comparison of the 2D and 3D cases.

Pos. no.	Dist. From belt [mm]	2D	3D
1	45	0.19	0.09
2	13	0.18	0.28
3	8	0.32	0.35

From the results presented in this thesis it is assumed that a 2D model with a refined surface mesh gives a good prediction of the temperature distribution within a cod fish during CBC-cooling. The comparison of the storage period was not as good, indicating that the boundary conditions were not accurate enough. One should, on the other hand, not neglect the 3D effects which cause heat extraction from the tail part of the cod. It should also be taken into account that the 3D model includes approximately six times the amount of elements than the 2D model. Hence the computational cost is greatly higher for the 3D model than the 2D model.

It is also interesting to see that when a CFD-simulation of the CBC-cooling is applied for 30 minutes and storage for one hour, the flesh temperature does not reach the initial freezing point of $T_{f,i} = -0.91^{\circ}\text{C}$, which is necessary for superchilling. It might therefore be assumed that a longer chilling period or a lower temperature should be applied for a fish of this size ($m \approx 2.5$ kg). A less time consuming process would be to process the fish to fillets which can be superchilled for a period of 6 to 8 minutes. A smaller fish, which has a mass closer to 1.5 kg, might be more suited for superchilling for 30 minutes, or perhaps just 14 minutes.

General errors in the CFD model, which might cause small effects on the results, are multiple and are listed below:

- The fish model geometry, including the contact area, is not exactly the same as of the measured fish.
- The inlet velocity and temperature in the CBC-cooler were not uniform.
- The period between the time when the fish was taken out of the CBC-cooler, put in the EPS box and the box closed was not modelled exactly.
- The exact position of the temperature data loggers, within the fish flesh, could not be precisely measured.
- During the storage period, two fish were put in each EPS box (see Figure 2.8(a)). The effects the two fish might have on each other were not taken into account in the CFD-model.

The results obtained in this study show that CFD modelling in terms of fluid flow and heat transfer has proven to be a realistic and functional tool to simulate superchilling of whole fish in a CBC-cooler. In future work CFD-modelling can be used to determine optimal values for parameters such as holding time, chilling temperature and air velocity.

Bibliography

- ANSYS. Ansys fluent 12.0 theory guide, 2009.
- M. G. Arnþórsdóttir, S. Arason, and B. Margeirsson. Combined blast and contact cooling: Effects on physiochemical characteristics of fresh haddock (*melanogrammus aeglefinus*) fillets. (Matís report 14-08), 2008.
- K. A. Fikiin. Ice content prediction methods during food freezing: a survey of the eastern european literature. *Journal of Food Engineering*, 1998.
- H. Gao. Methods of pre-cooling for fresh cod (*gadus morhua*) and influences on quality during chilled storage at -1.5°C . Technical report, The United Nations University: Fisheries Training Programme, 2007.
- E. Granryd. *Refrigerating Engineering - Part II*. Royal Institute of Technology, KTH, Stockholm, 2005.
- J. Holman. *Heat Transfer*. McGraw Hill, New York, 10 edition, 2010.
- M. iButton® Devices. ibutton products: ibuttons. <http://www.maxim-ic.com/products/ibutton/products/ibuttons.cfm>, 2011. Accessed August 10th, 2011.
- E. Instruments. 451126 - cfm/cmm vane anemometer datalogger. <http://www.extech.com/instruments/categories.asp?catid=1>, 2011. Accessed August 10th, 2011.
- W. A. Johnston, A. R. Nicholson, and G. D. Stroud. Freezing and refrigerated storage in fisheries, 1994. Accessed February 15th, 2012.

- H. L. Lauzon, B. Margeirsson, K. Sveinsdóttir, M. Guðjónsdóttir, M. G. Karlsdóttir, and E. Martinsdóttir. Overview on fish quality research. impact of fish handling, processing, storage and logistics on fish quality deterioration. *Matís report*, (39-10), 2010.
- J. H. Lienhard IV and J. H. Lienhard V. *A Heat Transfer Textbook*. Phlogiston Press, Cambridge Massachusets, fourth edition, 2010.
- H. Magnússon, H. L. Lauzon, K. Sveinsdóttir, B. Margeirsson, E. Reynisson, A. R. Rúnarsson, M. Guðjónsdóttir, K. A. Þórarinsdóttir, S. Arason, and E. Martinsdóttir. The effect of different cooling techniques and temperature fluctuations on the storage life of cod fillets (*gadus morhua*). *Matís report*, (23-09), 2009.
- B. Margeirsson, H. L. Lauzon, L. Þorvaldsson, S. V. Árnason, S. Arason, K. L. Valtýsdóttir, and E. Martinsdóttir. Optimised chilling protocols for fresh fish. *Matís report*, (54-10), 2010.
- B. Margeirsson, H. Pálsson, V. Popov, R. Gospavic, S. Arason, K. Sveinsdóttir, and M. Þór Jónsson. Numerical modelling of temperature fluctuations in superchilled fish loins packaged in expanded polystyrene and stored at dynamic temperature conditions. *International Journal of Refrigeration*, 2012.
- B. Margeirsson, R. Gospavic, H. Pálsson, S. Arason, and V. Popov. Experimental and numerical modelling comparison of thermal performance of expanded polystyrene and corrugated plastic packaging for fresh fish. 34(2):573–585, 2011.
- E. Martinsdóttir, K. Sveinsdóttir, J. Luten, R. Schelvis-Smit, and G. Hyldig. *Reference manual for the fish sector : Sensory evaluation of fish freshness*. QIM Eurofish, 2001.
- E. Martinsdóttir, B. Guðbjörnsdóttir, and H. L. Lauzon. Áhrif roðkælingar á gæði fiskflaka. (Icelandic Fisheries Laboratories-report 03-04), 2004.
- E. Martinsdóttir, B. Guðbjörnsdóttir, and H. L. Lauzon. Áhrif roðkælingar á gæði fiskflaka: Map-pökkuð og þídd. (Icelandic Fisheries Laboratories-report 10-05), 2005.
- E. Martinsdóttir, H. L. Lauzon, B. Margeirsson, K. Sveinsdóttir, L. Þorvaldsson, H. Magnússon, E. Reynisson, A. V. Jónsdóttir, S. Arason, and M. Eden. The effect of cooling methods at processing and use of gel-packs on storage life of cod (*gadus morhua*) loins - effect of transport via air and sea on temperature control and retail-packaging on cod deterioration. *Matís report*, (18-10), 2010.
- G. Olafsdóttir, H. L. Lauzon, E. Martinsdóttir, J. Oehlenschläger, and K. Kristbergsson. Evaluation of shelf life of superchilled cod (*gadus morhua*) fillets and the influence of temperature fluctuations during storage on microbial and chemical quality indicators. 2006.

- S. Rahman. *Food properties handbook*. CRC Press/Taylor Francis Group, 2009.
- C. Rha. *Theory, Determination and Control of Physical Properties of Food Materials*. Reidel Publishing, Dordrecht, Boston, 1975.
- K. L. Valtýsdóttir, B. Margeirsson, S. Arason, H. L. Lauzon, and E. Martinsdóttir. Guidelines for precooling of fresh fish during processing and choice of packaging with respect to temperature control in cold chains. *Matís report*, (40-10), 2010.
- E. W. Weisstein. Root mean square @ONLINE, 2012.
- F. M. White. *Viscous Fluid Flow*. McGraw - Hill, third edition, 2006.
- J. Zueco, F. Alhama, and C. G. Fernandez. Inverse determination of the specific heat of foods. *Journal of Food Engineering*, 64(3), 2004.

APPENDIX A

Test results from the project *Super-Chilled Round Fish - Pre Rigor*

Table A.1: Results from mass and length measurements of the fish used for the tests.

Test	Time [min]	m [kg]	L [cm]	L' [cm]
1	8	2.36	71	42
	10	1.45	57	32
	15	1.67	61	34
2	20	1.49	58	32
	25	2.87	75	44
3	8	2.51	70	39
	13	2.82	71	39
	18	2.72	67	39
4	15	1.49		
	30	1.46		
	15	3.44		
	30	3.67		
	0	1.72		

A.1 Test 1

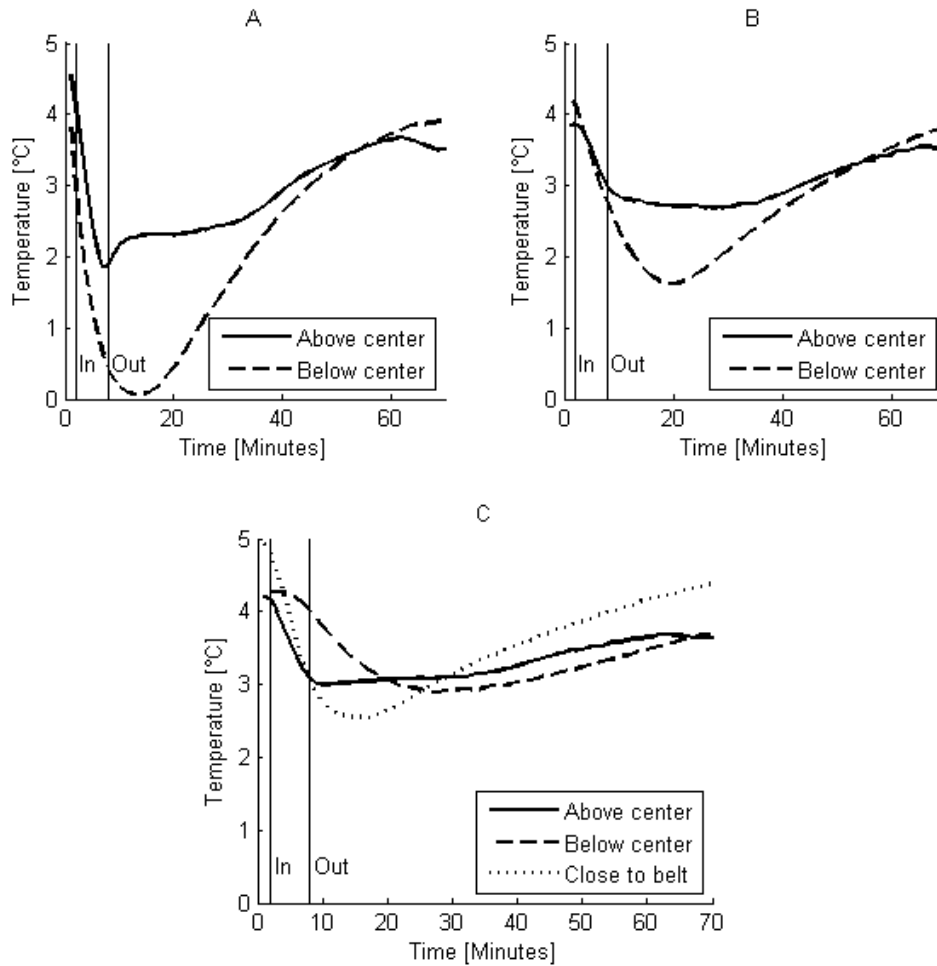


Figure A.1: Results at $T_{\infty} = -7.4^{\circ}\text{C}$ and CBC-cooling for 6 minutes, $m = 2.4$ kg.

Table A.2: Comparison of the lowest temperature values at different positions in the fish flesh after 8 minutes in the CBC-cooler.

	Position	T ₈ [°C]
A	Above	1.86
	Below	0.05
B	Above	2.69
	Below	1.62
C	Above	3.00
	Below	2.89
	Belt	2.55

Table A.3: Temperature at different positions in the fish flesh after 80 minutes.

	Position	T ₈₀ [°C]
A	Above	3.52
	Below	3.95
B	Above	3.55
	Below	4.04
C	Above	3.63
	Below	3.91
	Belt	4.55

A.2 Test 2

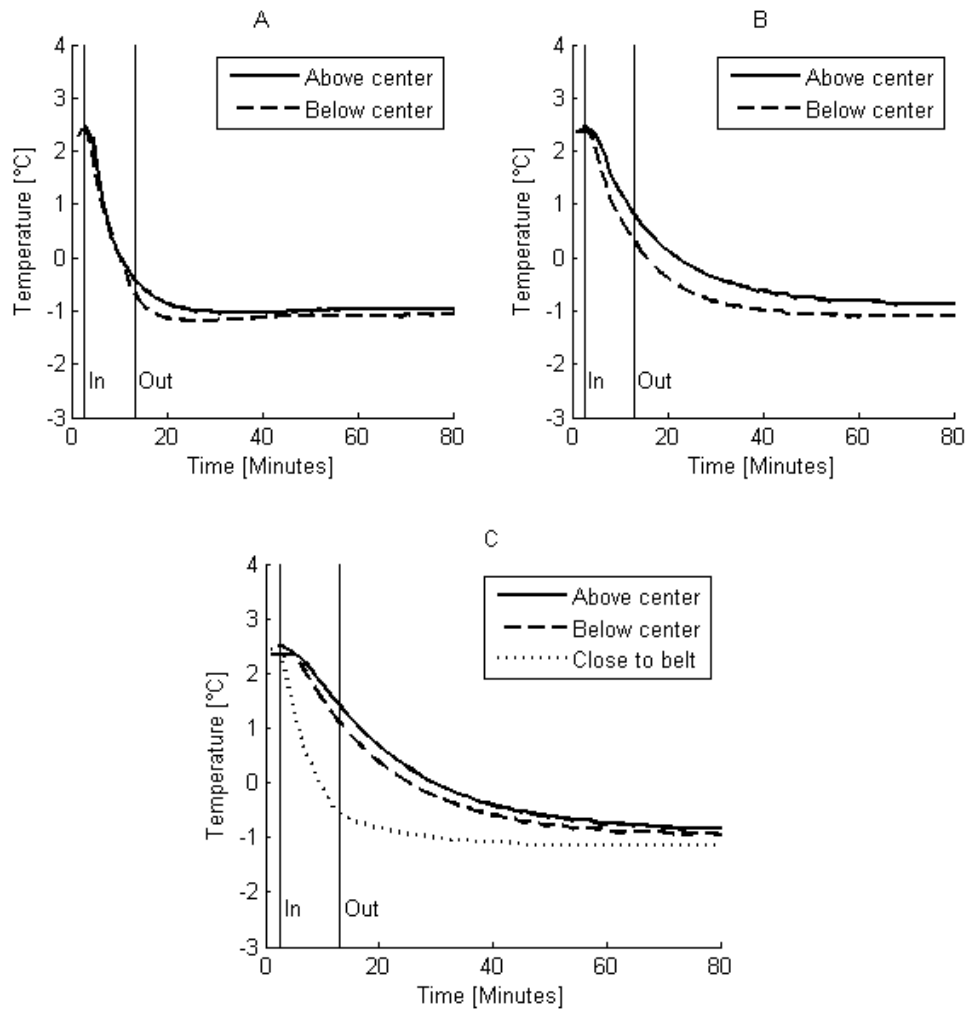


Figure A.2: Results at $T_{\infty} = -13.0^{\circ}\text{C}$ and CBC-cooling for 10 minutes, $m = 1.4$ kg.

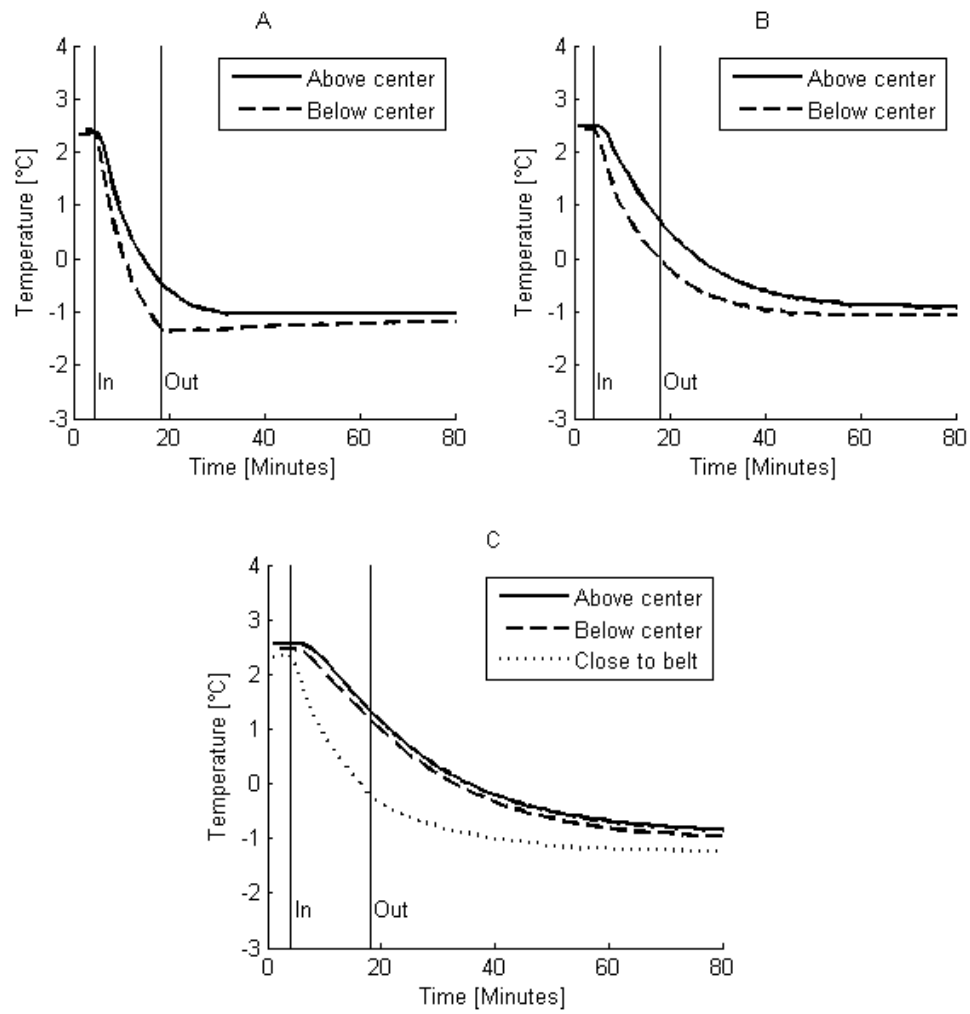


Figure A.3: Results at $T_{\infty} = -13.0^{\circ}\text{C}$ and CBC-cooling for 15 minutes, $m = 1.7\text{ kg}$.

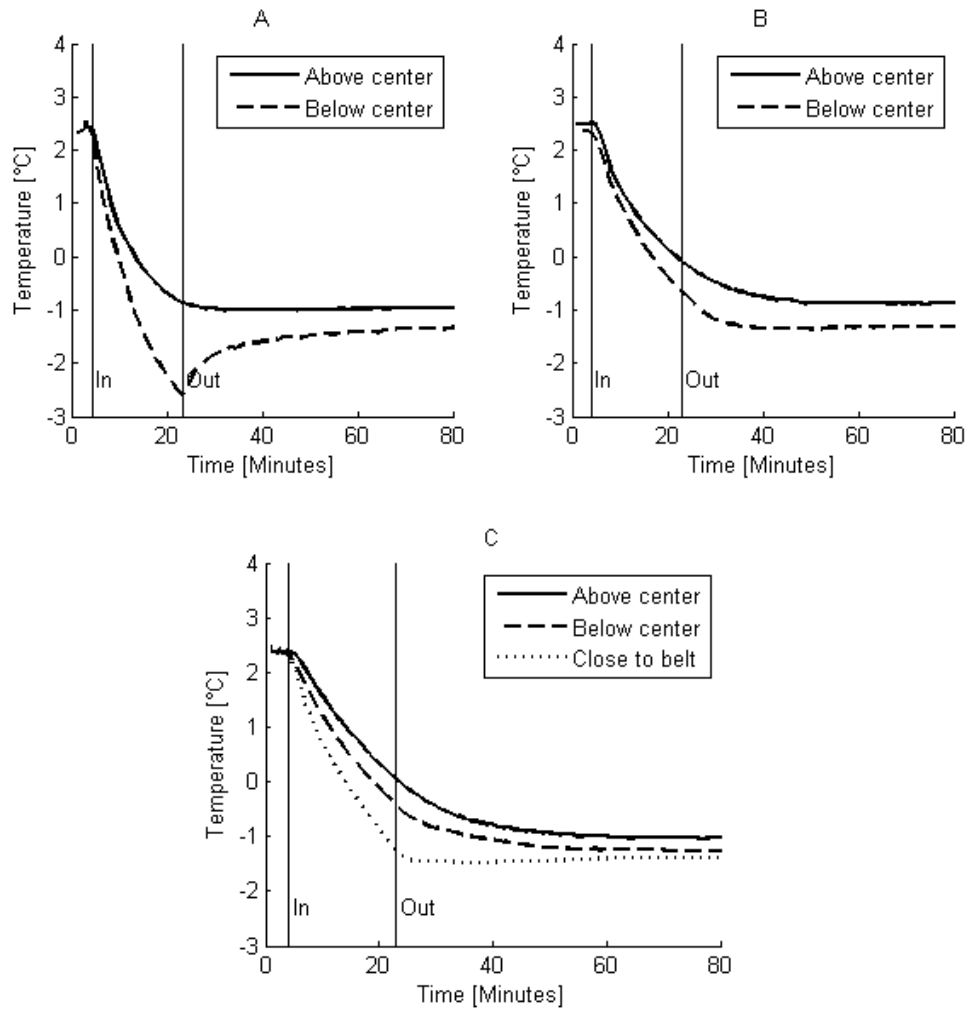


Figure A.4: Results at $T_{\infty} = -13.0^{\circ}\text{C}$ and CBC-cooling for 20 minutes, $m = 1.5\text{ kg}$.

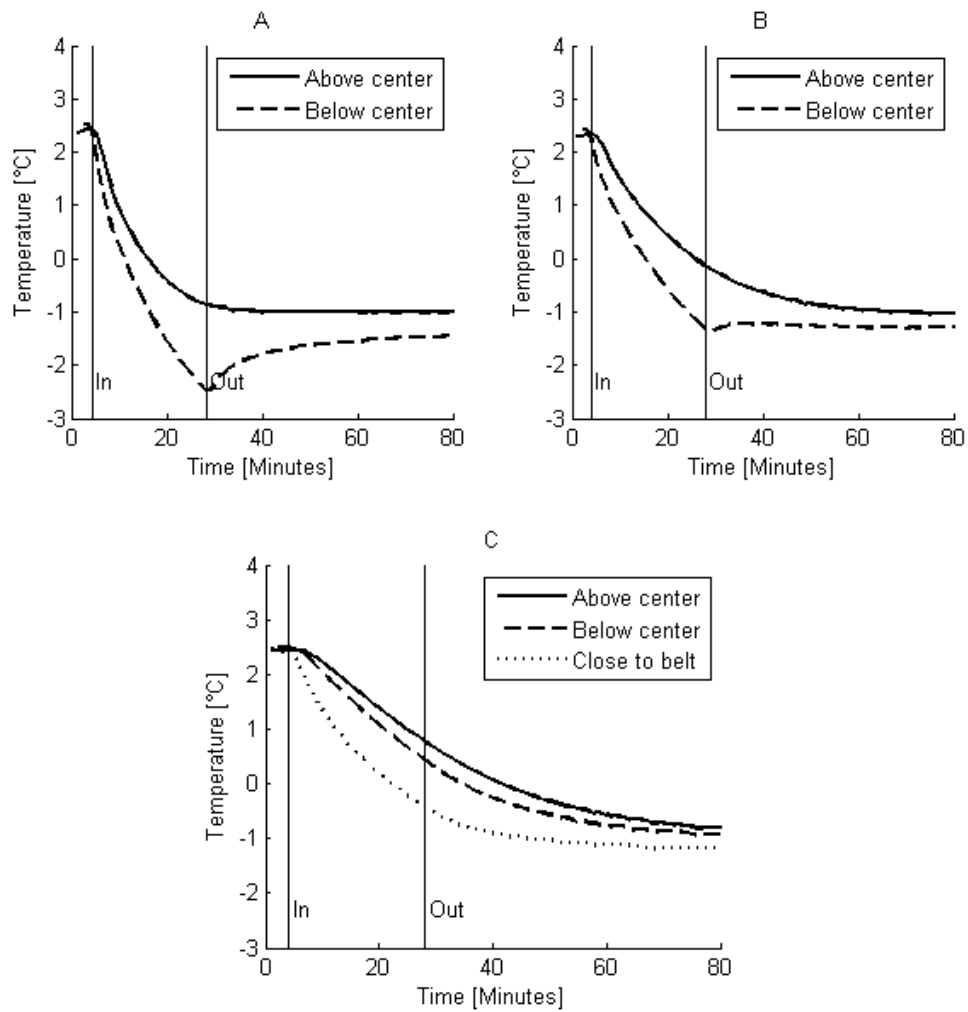


Figure A.5: Results at $T_{\infty} = -13.0^{\circ}\text{C}$ and CBC-cooling for 25 minutes, $m = 2.9\text{ kg}$.

Table A.4: *Lowest fish temperatures ($^{\circ}\text{C}$) at different positions for the four cooling durations in Test 2.*

	Position	10 min	15 min	20 min	25 min
A	Above	-1.04	-1.04	-1.01	-1.02
	Below	-1.19	-1.39	-2.59	-2.48
B	Above	-0.88	-0.92	-0.89	-1.04
	Below	-1.10	-1.07	-1.37	-1.38
C	Above	-0.91	-0.89	-1.04	-0.93
	Below	-0.97	-1.01	-1.26	-1.01
	Belt	-1.14	-1.24	-1.48	-1.22

Table A.5: *Comparison of the temperature values ($^{\circ}\text{C}$) at $t = 80$ min at different positions for the four cases.*

	Position	10 min	15 min	20 min	25 min
A	Above	-0.98	-1.04	-0.97	-1.01
	Below	-1.05	-1.19	-1.33	-1.45
B	Above	-0.88	-0.91	-0.88	-1.04
	Below	-1.10	-1.07	-1.32	-1.29
C	Above	-0.85	-0.85	-1.04	-0.82
	Below	-0.95	-0.97	-1.26	-0.94
	Belt	-1.13	-1.24	-1.38	-1.20

A.3 Test 3

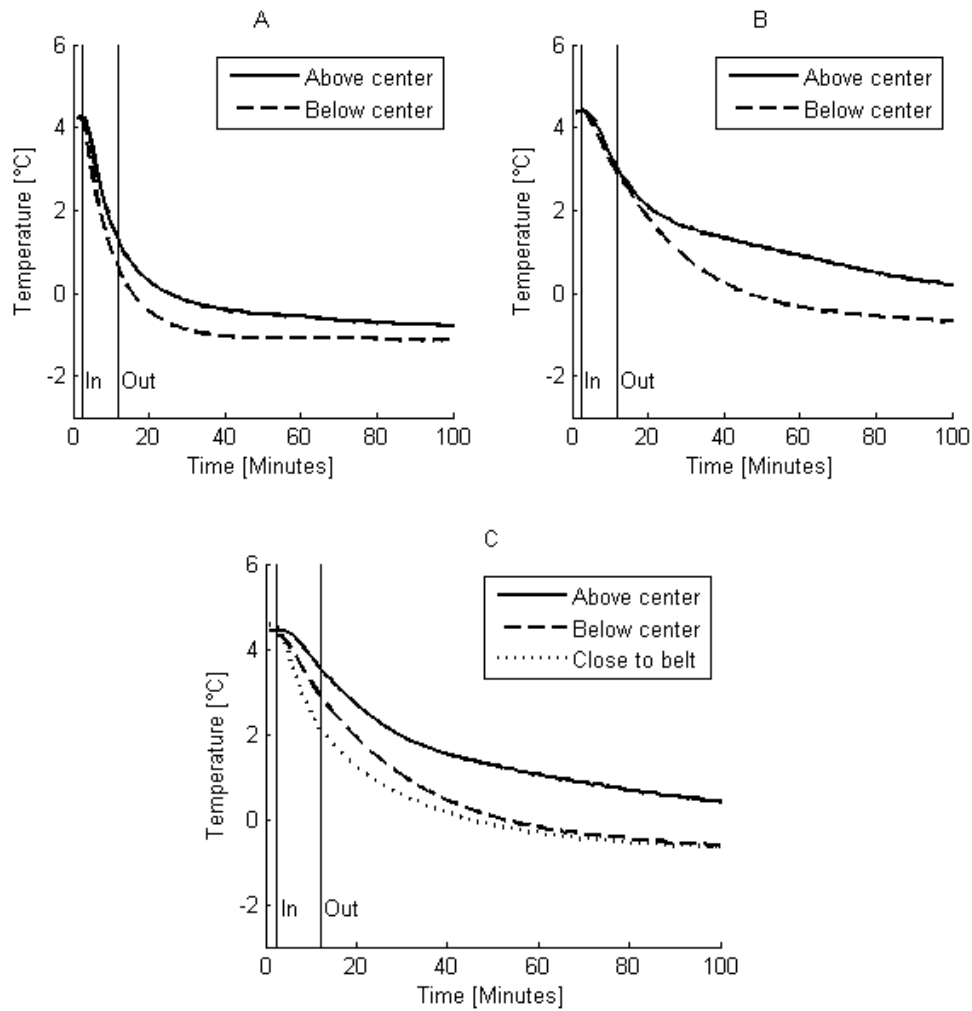


Figure A.6: Results at $T_{\infty} = -14.1^{\circ}\text{C}$ and CBC-cooling for 8 minutes, $m = 2.5$ kg.

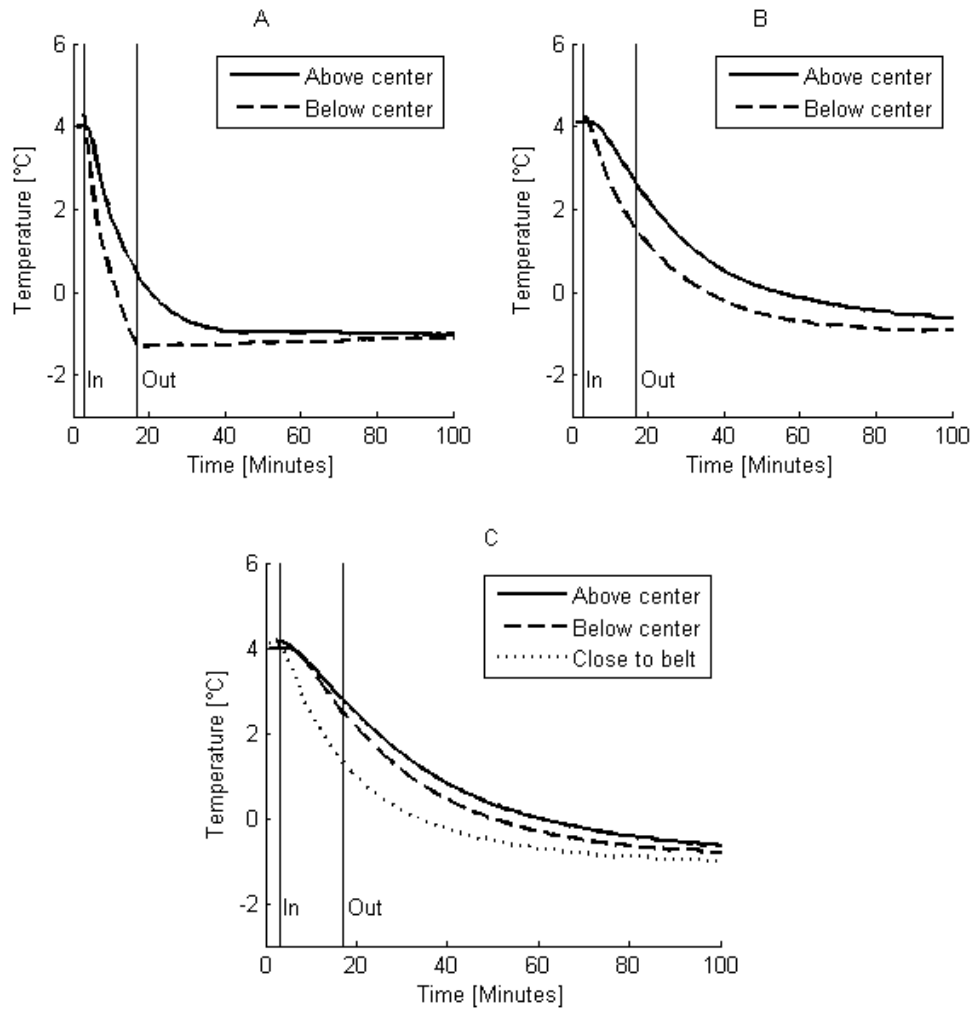


Figure A.7: Results at $T_{\infty} = -14.1^{\circ}\text{C}$ and CBC-cooling for 13 minutes, $m = 2.8\text{ kg}$.

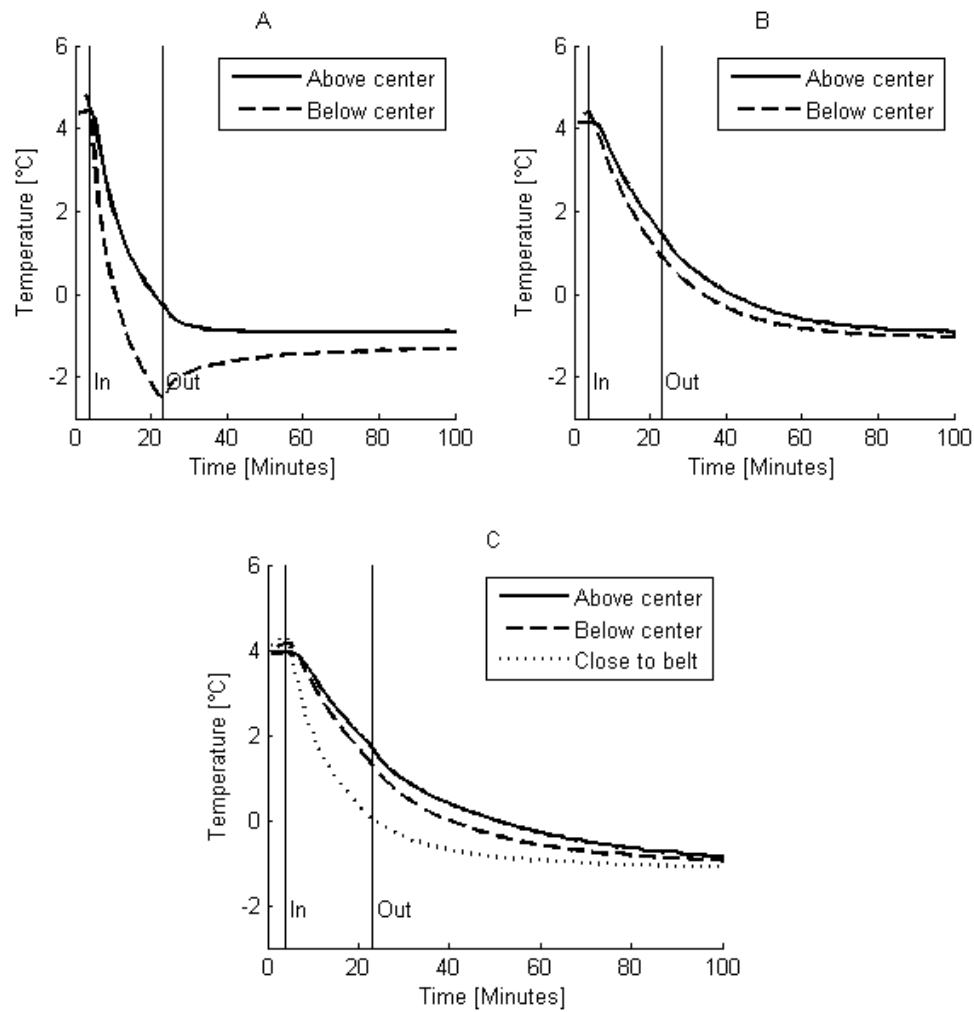


Figure A.8: Results at $T_{\infty} = -14.1^{\circ}\text{C}$ and CBC-cooling for 18 minutes, $m = 2.7\text{ kg}$.

Table A.6: Lowest fish temperatures ($^{\circ}\text{C}$) at different positions for the three cooling durations in Test 3.

	Position	8 min	13 min	18 min
A	Above	-0.91	-1.04	-0.91
	Below	-1.13	-1.32	-2.52
B	Above	-0.41	-0.82	-0.975
	Below	-0.89	-1.01	-1.07
C	Above	-0.17	-0.91	-1.04
	Below	-0.82	-0.94	-1.02
	Belt	-0.82	-1.07	-1.13

Table A.7: Comparison of the temperature values ($^{\circ}\text{C}$) at $t = 80$ min at different positions for the three cases.

	Position	8 min	13 min	18 min
A	Above	-0.72	-1.01	-0.91
	Below	-1.11	-1.14	-1.37
B	Above	0.48	-0.47	-0.82
	Below	-0.53	-0.88	-1.01
C	Above	0.68	-0.41	-0.66
	Below	-0.45	-0.65	-0.83
	Belt	-0.56	-0.91	-1.07

A.4 Test 4

Table A.8: Test groups in Test 4 at $T_{\infty} = -13.6^{\circ}\text{C}$. Number of fish in each group: 2.

Group nr.	Mass [kg]	Cooling time [min]
1	1.5	15
2	1.5	30
3	3.4	15
4	3.7	30
5	1.7	0 (reference group)

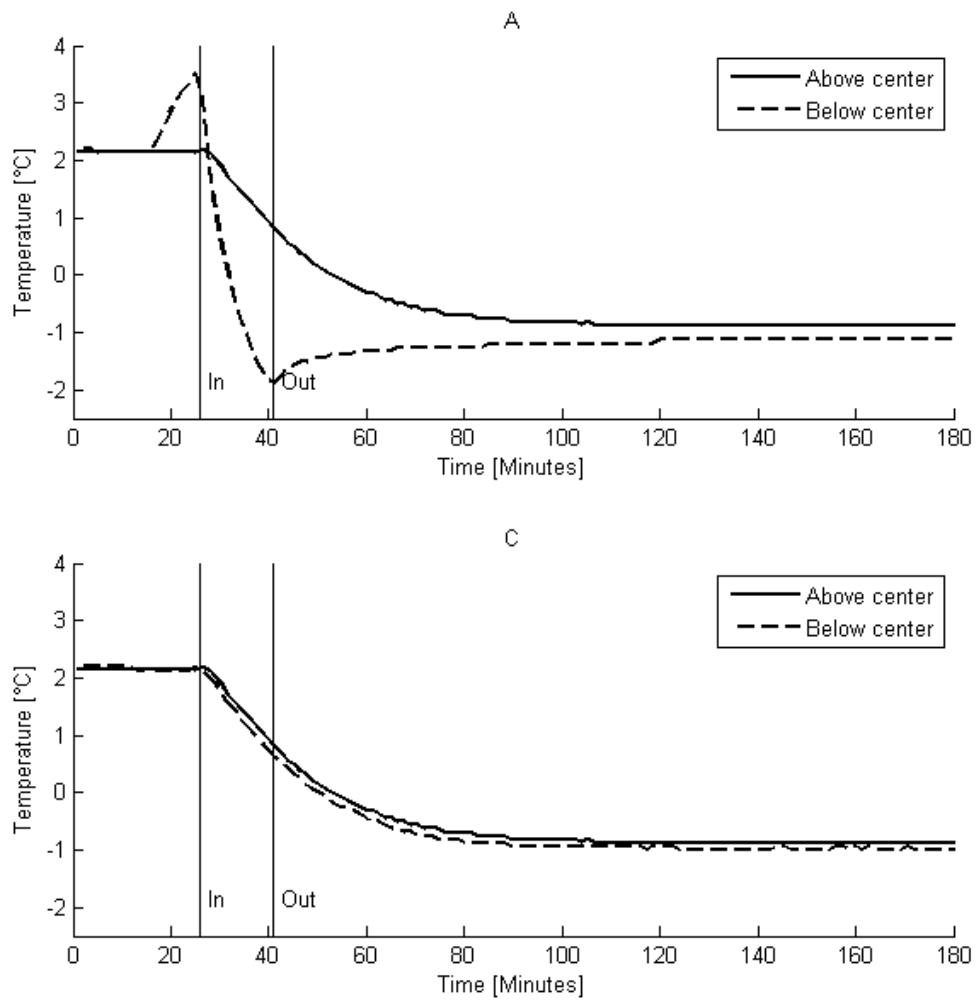


Figure A.9: Temperature results for CBC-cooling of group 1 at $T_{\infty} = -13.6^{\circ}\text{C}$, $m = 1.5\text{ kg}$.

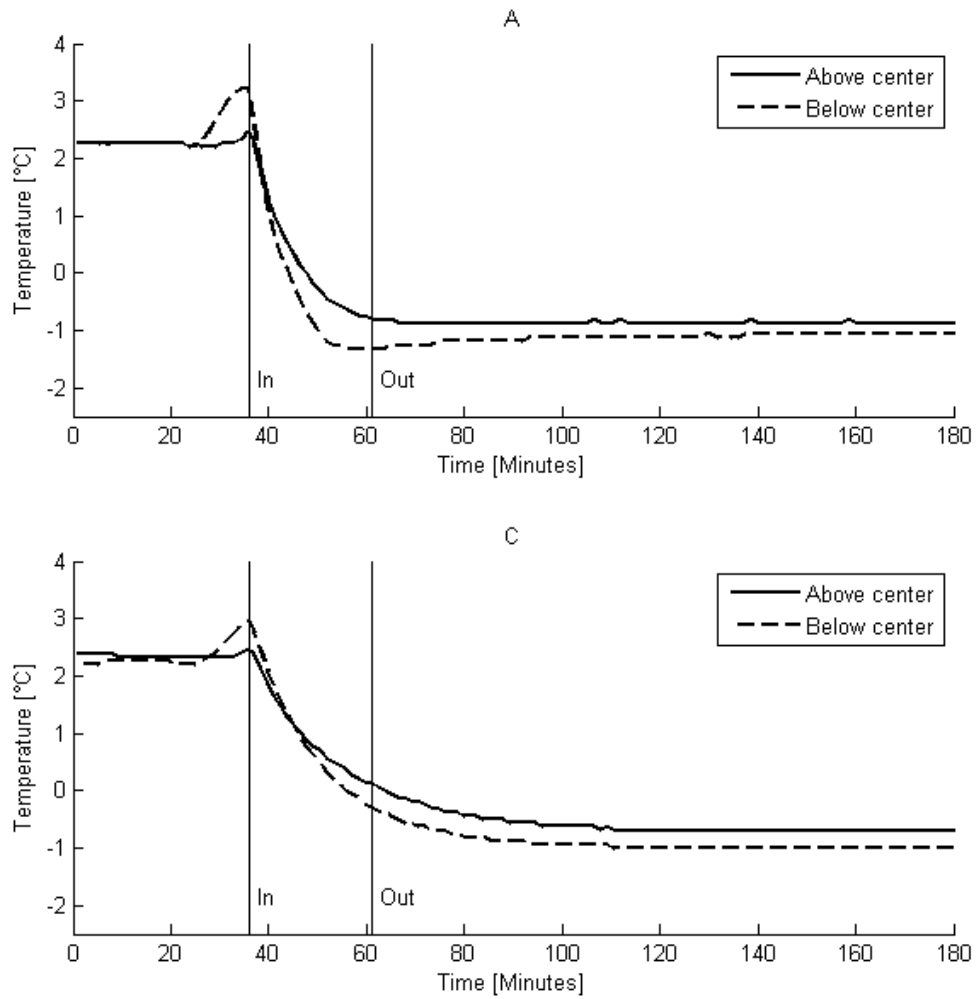


Figure A.10: Temperature results for CBC-cooling of group 2 at $T_{\infty} = -13.6^{\circ}\text{C}$, $m = 1.5\text{ kg}$.

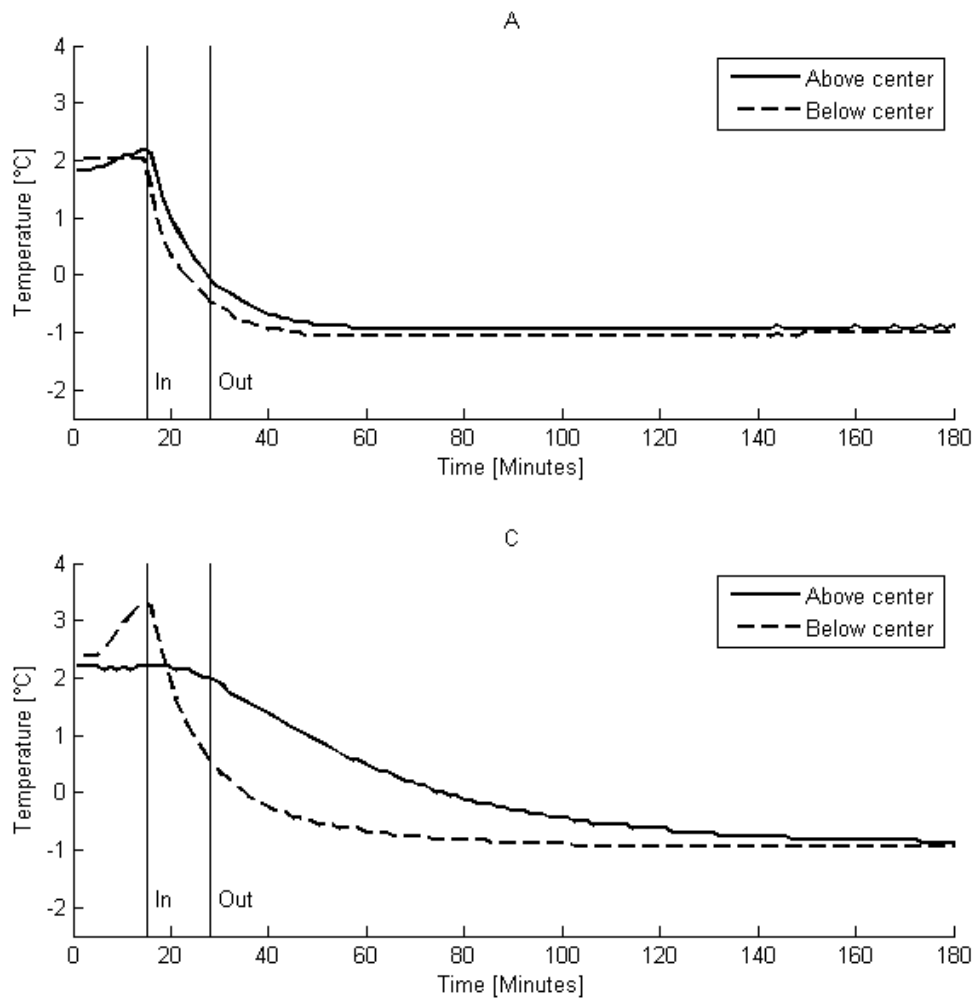


Figure A.11: Temperature results for CBC-cooling of group 3 at $T_{\infty} = -13.6^{\circ}\text{C}$, $m = 3.4\text{ kg}$.

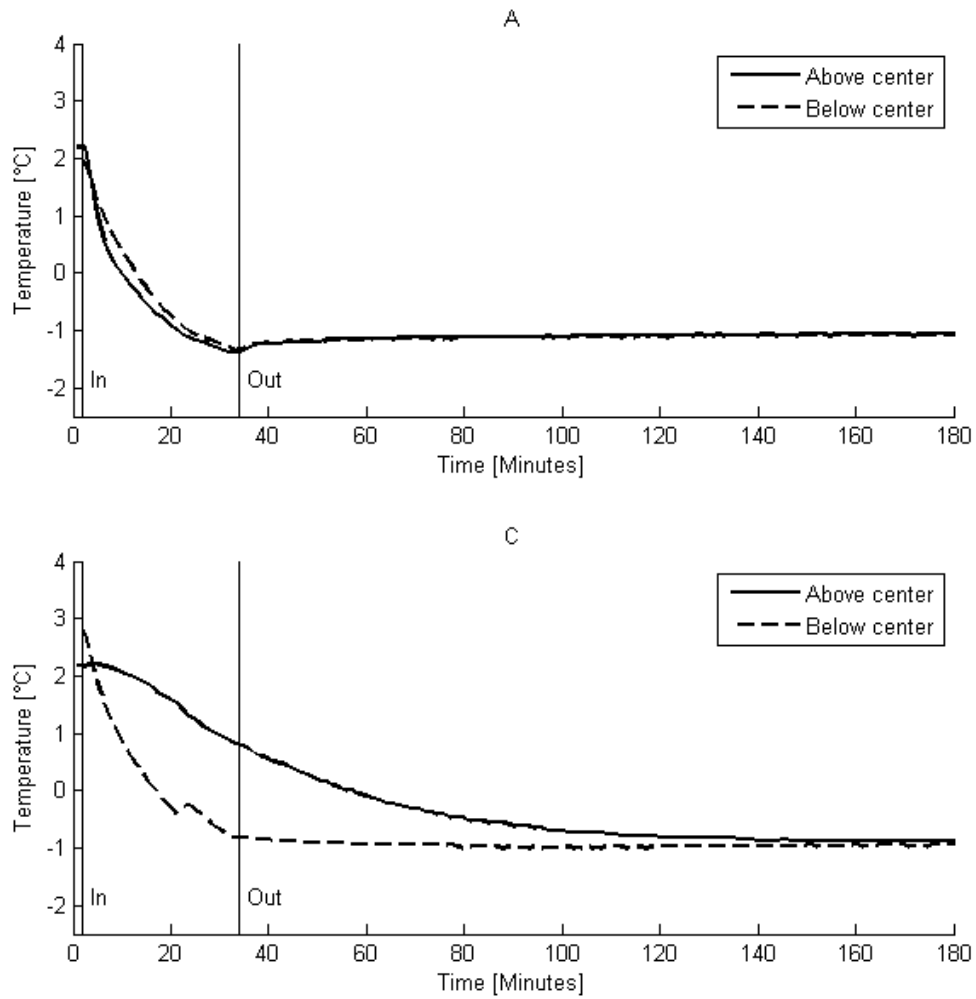


Figure A.12: Temperature results for CBC-cooling of group 4 at $T_{\infty} = -13.6^{\circ}\text{C}$, $m = 3.7\text{ kg}$.

Table A.9: Lowest temperature values ($^{\circ}\text{C}$) in groups 3 and 4 for 15 and 30 minutes of CBC-cooling, respectively, in Test 4.

		Time [min]/Group no.			
Position		15/1	30/2	15/3	30/4
A	Above	-0.88	-0.88	-0.94	-1.38
	Below	-1.89	-1.32	-1.07	-1.35
C	Above	-0.88	-0.69	-0.88	-0.88
	Below	-1.00	-1.01	-0.94	-1.01

A.4.1 Storage at Matis

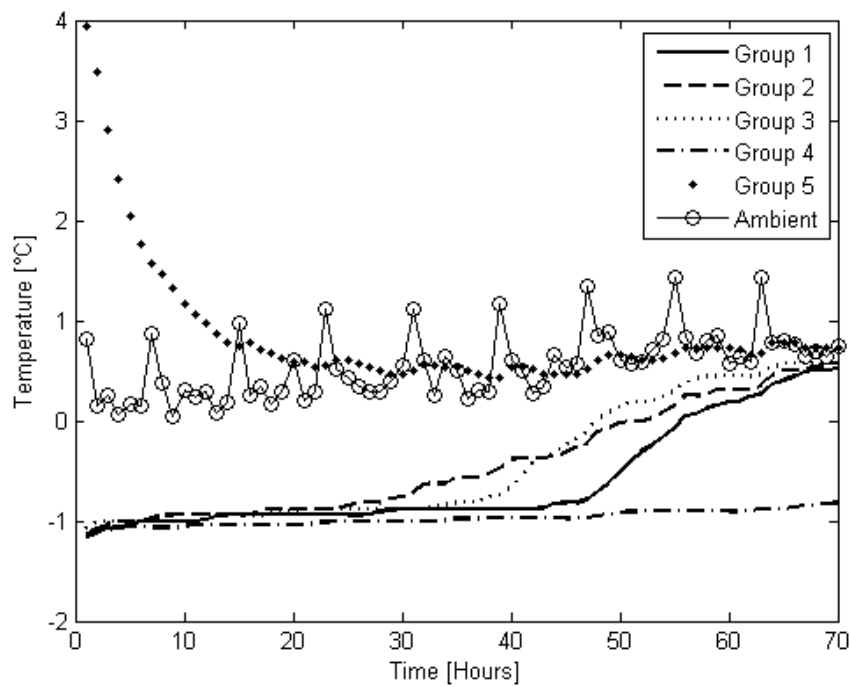


Figure A.13: Temperature in cross section A during chilled storage at Matis following Test 4.

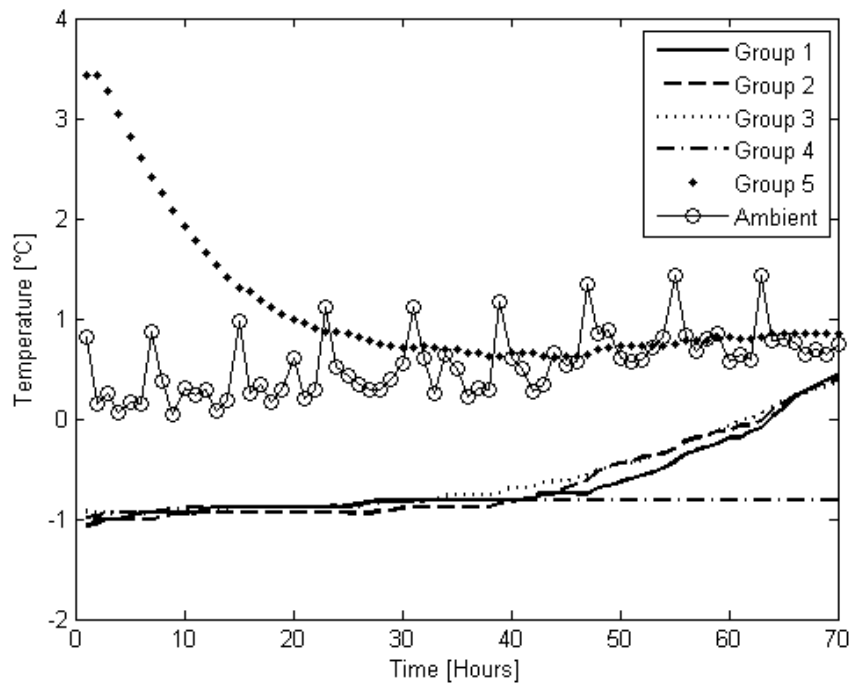


Figure A.14: Temperature in cross section C during chilled storage at Matis following Test 4.

DTU Mechanical Engineering
Section of Fluid Mechanics, Coastal and Maritime Engineering
Technical University of Denmark

Nils Koppels Allé, Bld. 403
DK- 2800 Kgs. Lyngby
Denmark
Phone (+45) 45 25 13 60
Fax (+45) 45 88 43 25

www.mek.dtu.dk